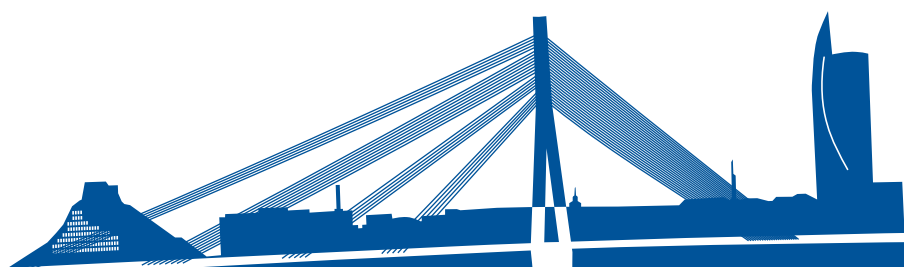


DEVELOPMENTS in ptics and Communications 2015

Book of Abstracts



Riga, Latvia, April 8 – 10, 2015

11th International Young Scientist conference

Developments in Optics and Communications 2015

Book of Abstracts

Editor:

Janis Zaharans

Institute of Atomic Physics and Spectroscopy

University of Latvia

Skunu street 4, Riga, LV1050, Latvia

e-mail: janis.zaharans@gmail.com

Assistant Editor:

Martins Bruvelis

Faculty of Physics and Mathematics

University of Latvia

Zellu street 8, Riga, LV1002, Latvia

e-mail: martins.bruvelis@gmail.com

URL: <https://plus.google.com/+MartinsBruvelis>

ISBN: 978-9934-517-80-8

e-ISBN: 978-9934-517-81-5

© 2015 University of Latvia, J. Zaharans, M. Bruvelis

This work is subject to copyright. All rights are reserved. This work may not be translated or copied in whole or in part without the written permission of the publisher (University of Latvia, J. Zaharans, M. Bruvelis).

Cover design: M. Bruvelis, E. Linina, Riga

www.docriga.lv

1 Welcome

The Organizing Committee kindly welcomes you to the 11th International Young Scientist conference “Developments in Optics and Communications 2015”. This conference is organized by University of Latvia SPIE student chapter (UL SPIE), OSA Latvian student chapter and University of Latvia Young Minds Section.

Henry Ford once said: “Coming together is a beginning; keeping together is progress; working together is success.” There’s no doubt that science requires team work and sharing ideas.

That’s why the purpose of this conference is to bring together students and young scientists who are working experimentally and theoretically in the fields of optics and photonics to share and exchange new ideas and to establish contacts for future collaboration. The conference is a good way how to encourage students of physics to train their soft skills and present their BSc, MSc or PhD thesis.

The young scientist conference has been evolving successfully for the past years. The conference traditionally features invited and contributed talks in four sections:

- Laser physics and spectroscopy;
- Biophotonics;
- Optical materials and phenomena;
- Vision science.

1.1 OSA-UL Best student presentation prize

We are delighted to announce that OSA-UL Best student presentation prize will be awarded to the best contributed talk and to the best poster presented at the conference. The talk/poster must be produced and presented by a student. The prize jury consists of members of ULSPIE and OSA-UL. The winners of the prize will be announced during the award ceremony at the end of the conference. The prize consists of a diploma and 50 € in cash.

Evaluation criteria for oral and poster presentations are published on the conference web page www.docriga.lv.

1.2 The Organizing Committee

1.2.1 DOC Chairs

- **Marta Lange**
PhD student
Institute of Atomic Physics and Spectroscopy, University of Latvia
- **Janis Smits**
MSc student
University of Latvia

1.2.2 Organizers

- **Alise Kalteniece**
Optometrist
Latvian American Eye Center
- **Arturs Bundulis**
MSc student
Institute of Solid State Physics,
University of Latvia
- **Arturs Cinins**
PhD student
Institute of Atomic Physics and
Spectroscopy, University of
Latvia
- **Brigita Zutere**
MSc student
Faculty of Biology, University of
Latvia
- **Elza Linina**
BSc student
Institute of Solid State Physics,
University of Latvia
- **Ilze Oshina**
BSc student
Faculty of Physics and Mathe-
matics, University of Latvia
- **Inesa Ferulova**
PhD student
Institute of Atomic Physics and
Spectroscopy, University of
Latvia
- **Inga Saknīte**
PhD student, Researcher
Biophotonics Laboratory
Institute of Atomic Physics and
Spectroscopy, University of
Latvia
- **Janis Zaharans**
MSc student
Institute of Atomic Physics and
Spectroscopy, University of
Latvia
- **Lasma Asare**
PhD student
Institute of Atomic Physics and
Spectroscopy, University of
Latvia
- **Martins Zeidaks**
Institute of Technical Physics,
Riga Technical University
- **Matiss Lacis**
BSc student
Institute of Biomedical Engineer-
ing and Nanotechnologies, Riga
Technical University
- **Varis Karitans**
Leading researcher
Institute of Solid State Physics,
University of Latvia

1.2.3 Scientific committee

- **Dr. Habil. Phys. Andris Sternbergs**
Institute of Solid State Physics, University of Latvia
- **Prof. Janis Spigulis**
Institute of Atomic Physics and Spectroscopy, University of Latvia
- **Prof. Ruvins Ferber**
Faculty of Physics and Mathematics, University of Latvia
- **Prof. Maris Ozolins**
Department of Optometry and Vision science, University of Latvia

2 Program. Day 1 & 2

Wednesday, 8th April			Thursday, 9th April			
08:45 - 09:00	Registration		08:45 - 09:00	IN04 Invited: Florian Gahbauer		
09:00 - 09:20						
09:20 - 09:40	Opening session		09:20 - 09:40	Optical Materials and Phenomena (OptMat) contributed talks		
09:40 - 10:00			09:40 - 10:00			C01
10:00 - 10:20	Coffee break		10:00 - 10:20			C02
10:20 - 10:40	IN01	Invited: Aivars Vembris	10:20 - 10:40			C03
10:40 - 11:00			10:40 - 11:00	C04		
11:00 - 11:20	A01	Laser Physics and Spectroscopy (LasPh) contributed talks	11:00 - 11:20	C05	Coffee break	
11:20 - 11:40	A02		11:20 - 11:40			
11:40 - 12:00	A03		11:40 - 12:00	P01 - P17	Poster session, part I	
12:00 - 12:20	A04		12:00 - 12:20			
12:20 - 12:40	Lunch		12:20 - 12:40			
12:40 - 13:00			12:40 - 13:00			
13:00 - 13:20	IN02	Invited: Dainis Jakovels	13:00 - 13:20			
13:20 - 13:40			13:20 - 13:40			
13:40 - 14:00	IN03	Invited: Lise Lyngsnes Randeberg	13:40 - 14:00			
14:00 - 14:20			14:00 - 14:20	Lunch		
14:20 - 14:40	B01	Biophotonics (BioPhot)	14:20 - 14:40			
14:40 - 15:00	Short break		14:40 - 15:00			
15:00 - 15:20	B02	Biophotonics (BioPhot) contributed talks	15:00 - 15:20			
15:20 - 15:40	B03		15:20 - 15:40			
15:40 - 16:00	B04		15:40 - 16:00			
16:00 - 16:20	B05		16:00 - 16:20			
16:20 - 16:40	B06		16:20 - 16:40	Tour to Old Riga		
16:40 - 17:00			16:40 - 17:00			
17:00 - 17:20	Welcome party		17:00 - 17:20			
17:20 - 17:40			17:20 - 17:40			
17:40 - 18:00			17:40 - 18:00			
18:00 - 18:20			18:00 - 18:20			
18:20 - 18:40			18:20 - 18:40			
18:40 - 19:00			18:40 - 19:00			
19:00 - 19:20					19:00 - 19:20	
19:20 - 19:40			19:20 - 19:40			
19:40 - 20:00			19:40 - 20:00			

3 Program. Day 3

Friday, 10th April		
08:45 - 09:00		
09:00 - 09:20	IN05	Invited: Pablo Artal
09:20 - 09:40		
09:40 - 10:00	D01	Vision Science contributed talks
10:00 - 10:20	D02	
10:20 - 10:40	D03	
10:40 - 11:00	D04	
11:00 - 11:20	IN06	Invited: Evija Gulbinska
11:20 - 11:40		
11:40 - 12:00	Coffee break	
12:00 - 12:20	P18 - P33	Poster session, part II
12:20 - 12:40		
12:40 - 13:00		
13:00 - 13:20		
13:20 - 13:40		
13:40 - 14:00		
14:00 - 14:20	Lunch	
14:20 - 14:40		
14:40 - 15:00	IN07	Invited: Jurita Kruma Presentation Skill Workshop
15:00 - 15:20		
15:20 - 15:40		
15:40 - 16:10		
16:10 - 16:20	Closing session	
16:20 - 16:40		
16:40 - 16:50		
16:50 - 17:20		
17:20 - 17:40		
17:40 - 18:00		
18:00 - 18:20		
18:20 - 18:40		
18:40 - 19:00		
19:00 - 19:30		
19:30 - 20:00		
20:00 - ...	After-party in Latvian "Zaķišu pirtīņa"	

Detailed Program & Schedule

1	Welcome	vi
1.1	OSA-UL Best student presentation prize	vi
1.2	The Organizing Committee	vii
1.2.1	DOC Chairs	vii
1.2.2	Organizers	vii
1.2.3	Scientific committee	viii

2	Program. Day 1 & 2	ix
----------	-------------------------------	-----------

3	Program. Day 3	x
----------	-----------------------	----------

	Detailed Program & Schedule	xi
--	--	-----------

	Wednesday, April 8, 2015	1
--	---------------------------------	----------

08:45 - 09:20 Registration

09:20 - 10:00 Opening session

10:00 - 10:20 Coffee break

	(LasPhys) Laser physics and spectroscopy	1
--	---	----------

Invited talk

10:20 - 11:00	<u>Aivars Vembris</u> Organic solid state lasers	1
----------------------	---	----------

11:00 - 11:20	<u>Sergey Sychugin</u> Terahertz Cherenkov radiation from focused laser pulses	2
----------------------	---	----------

11:20 - 11:40	<u>Elena Svinkina</u> Asymmetric terahertz Cherenkov radiation in LiNbO ₃	3
----------------------	---	----------

11:40 - 12:00	<u>Esben Larsen</u> Ellipticity Dependence of High-order Harmonics Generation	4
----------------------	--	----------

12:00 - 12:20	<u>Artis Kruzins</u> Fourier-transform spectroscopy studies and deperturbation analysis of $A^1\Sigma^+$ and $b^3\Pi$ states in RbCs	5
----------------------	---	----------

12:20 - 13:00 Lunch break

Invited talk**13:00 - 13:40** Dainis Jakovels

Applications of airborne optical remote sensing techniques for environmental assessment and monitoring 6

Invited talk**13:40 - 14:20** Lise Lyngsnes Randeberg

How do optical properties affect light transport in tissue, and which parameters do you need to care about in the lab? 7

14:20 - 14:40 Tatevik Chalyan

Performance optimisation of biosensors based on SiON microring resonators 8

14:40 - 15:00 **Short break****15:00 - 15:20** Aleksandra Zhelyazkova

Polarization-Sensitive Synchronous Fluorescence Spectroscopy of Human Basal Cell Carcinoma 9

15:20 - 15:40 Roberts Kadikis

Method for registration of multispectral skin images 10

15:40 - 16:00 Inga Saknite

Estimation of rosacea treatment effectiveness by RGB imaging . 11

16:00 - 16:20 Jacob Renzo Bauer

Spectral reflectance estimation with an optical non contact device for skin assessment 12

16:20 - 16:40 Steven Beekmans

Development of a Fiber-top Controlled Adaptable Stiffness Needle 13

17:00 - ... **Welcome party**

Thursday, April 9, 2015	13
(OptMat) Optical materials and phenomena	13
Invited talk	
09:00 - 09:40 <u>Florian Helmuth Gahbauer</u> Nitrogen Vacancy Centers in Diamonds for Sensing and Quantum Information	13
9:40 - 10:00 <u>Inga Jonane</u> Temperature dependence of the local structure of Y_2O_3 from EX- AFS analysis using evolutionary algorithm method	15
10:00 - 10:20 <u>Guna Doke</u> Impact of oxygen related defects on the properties of up-conversion luminescence of $NaLaF_4:Er^{3+}$ material	16
10:20 - 10:40 <u>Krista Klismeta</u> Azobenzene containing molecular glass as an optical recording material	17
10:40 - 11:00 <u>Martins Narels</u> Amplified spontaneous emission of DCM derivative in PVK thin film.	18
11:00 - 11:20 <u>Marija Duncce</u> Photoluminescence in Er^{3+} -doped $0.4Na_{0.5}Bi_{0.5}TiO_3-(0.6-x)SrTiO_3-$ $xPbTiO_3$ solid solutions	19
11:20 - 11:40 Coffee break	
Poster session	20
11:40 - 14:00 Poster session, part I	
P01 <u>Gatis Tunens</u> Modeling absorption spectrum of skin in the near-infrared spec- tral range by Monte Carlo simulations	20
P02 <u>Ilze Oshina</u> Snapshot mapping of skin chromophores at triple-wavelength il- lumination	21
P03 <u>Vitali Ghoghoberidze</u> Numerical calculation of DOS in nanograting layers using method of auxiliary sources	22

P04	<u>Meldra Kemere</u> Luminescence studies of europium and coactivator doped oxyflu- oride glasses and glass ceramics	24
P05	<u>Edite Paule</u> HD 50975: a yellow supergiant in a spectroscopic binary system	25
P06	<u>Inga Brice</u> GNSS – More Than A Simple Tool For Navigation	26
P07	<u>Andris Berzins</u> Magnetic field imaging using nitrogen vacancy (NV) centres in a diamond lattice	27
P08	<u>Inese Birzniece</u> High resolution laser spectroscopy and potential construction of the low-lying $^1\Pi$ electronic states in KCs and RbCs molecules . .	28
P09	<u>Daiga Cerane</u> Comparison of optimized and most significant illuminants using a spectrally tunable light source	29
P10	<u>Karola Panke</u> Accommodation lag under monocular and binocular conditions in symptomatic and asymptomatic emmetropes	30
P11	<u>Beata Marcinkevica</u> The perception of coherent motion for the centric and eccentric fixation of a stimulus	31
P12	<u>Diana Bete</u> Influence of mental fatigue on visual grouping task	33
P13	<u>Jazeps Rutkis</u> Dust particle laser detection in laboratory air	34
P14	<u>Maris Ozolinsh</u> Smart model eye on base of polymer dispersed liquid crystals and CMOS sensor	35
P15	<u>Zane Jansone</u> "Variantor" functional spectral filter that stimulates trichromats see as dichromats	36
P16	<u>Astghik Kuzanyan</u> High Speed Single Photon Detector	37

P17	<u>Andris Antuzevics</u> EPR investigation of Gd^{3+} local structure in ScF_3	38
14:00 - 15:00 Lunch break		
16:20 Tour to Old Riga		
Friday, April 10, 2015		39
(VisSci) Vision science		39
Invited talk		
09:00 - 09:40	<u>Pablo Artals</u> Adaptive optics for better vision	39
9:40 - 10:00	<u>Varis Karitans</u> Measurement of the thickness of the corneal tear-film using a Twyman-Green interferometer	40
10:00 - 10:20	<u>Janis Baltraitis</u> Axial eye elongation and changes in refraction error for myopic European children using custom-made overnight orthokeratology contact lenses	41
10:20 - 10:40	<u>Sergejs Fomins</u> System for melanopsin related pupillometry	42
10:40 - 11:00	<u>Ilze Laicane</u> Perception of biological motion in central and peripheral visual field	43
Invited talk		
11:00 - 11:40	<u>Evija Gulbinska</u> Visian ICL: intraocular collamer lens for refractive correction . .	44
11:40 - 12:00 Coffee break		
Poster session		45
12:00 - 14:30 Poster session, part II		
P18	<u>Inna Burkova</u> Estimation of the effect of Cs and Sr salts on <i>Brassica napus</i> L. CFI parameters using "Floratest" optical biosensor	45

P19	<u>Antra Dzerve</u> Investigation of skin autofluorescence lifetime under optical irradiation	46
P20	<u>Julija Pervenecka</u> Optical and photoelectrical properties of DMABI chromophore consisting molecules	47
P21	<u>Olga Kiselova</u> Properties of zinc oxide thin films synthesized by extraction-pyrolytic method	48
P22	<u>Arturs Mozers</u> Alignment-to-orientation conversion due to hyperfine Paschen-Back type angular momentum decoupling in atomic rubidium .	49
P23	<u>Madara Zinge</u> Spectroscopic studies of cadmium containing high frequency electrodeless light sources	50
P24	<u>Mateusz Szatkowski</u> Optical vortex trajectory inside the beam focused by an axicon .	51
P25	<u>Evija Ziba</u> Impact of fatigue on spatial language and cognition	52
P26	<u>Elina Vevere</u> Speeded verification test in spatial perception under mental fatigue condition	53
P27	<u>Liva Arente</u> Impact of mental fatigue on perception of biological motion . .	54
P28	<u>Anete Pausus</u> The effect of blur adaptation on blur sensitivity	55
P29	<u>Kristiana Ozola</u> Mental rotation test in condition of fatigue	56
P30	<u>Renars Truksa</u> Experiment session duration effect on chromatic sensitivity threshold	57
P31	<u>Inga Jurcinska</u> The Effect of Fatigue on Eye Movements and Metaphor Comprehension in Reading	58

P32	<u>Ingrida Lavrinovica</u> Investigation of EDFA performance in 8 channel WDM transmission system.	59
P33	<u>Piyush Bajpayee</u> Dispersion influence considerations in fiber optics transmission system	60
14:00 - 14:40	Lunch break	
14:40 - 16:10	Presentation Skills Workshop	
16:10 - 16:50	Closing session	
20:00 - ...	After-party in Latvian "Zaķišu pirtiņa"	

Notes	60
--------------	-----------

Organic solid state lasers

Aivars Vembris

Institute of Solid State Physics, University of Latvia, 8 Kengaraga Str., Riga, LV 1063, Latvia

E-mail: aivars.vembris@cfi.lu.lv,

First LASER (Light Amplification by Stimulated Emission of Radiation) was discovered in 1960. Ruby laser which works in pulse regime was invented first. At the end of the year was shown first continuous wave laser which active material was helium-neon gas. After half a year lasers experienced its commercialization. In further years lasers become more efficient and powerful.

First laser where organic compounds was used as active medium were invented in 1966 by P. P. Sorokin and F. P. Schäfer. Dye laser active medium consists from laser dyes dissolved in organic solvent. One of the mane advantages of such laser was tuning of wavelength which is very important for selective interaction with investigated material. Disadvantage of such laser is complex maintenance.

Presentation will be divided in two parts. First part will be about development of dye and solid state organic lasers and issues which still should be addressed. In the second part will be presented achievements of Laboratory of Organic Materials related to organic solid state lasers.

Terahertz Cherenkov radiation from focused laser pulses

Sychugin S.A.^{*}, Bakunov M.I.

University of Nizhny Novgorod, 23 Gagarin Ave., Nizhny Novgorod, Russia, 603950

^{*}E-mail: ssychugin@gmail.com

Cherenkov radiation of terahertz waves by a femtosecond laser pulse propagating in an electro-optic crystal was proposed as a way of terahertz generation about 30 years ago [1]. In [1] and numerous later papers, the effect has been thoroughly studied theoretically in the assumption that the laser pulse propagates without changing its shape. In a typical experiment, however, strong focusing of the pump laser beam is used to provide a high optical intensity required for nonlinear optical rectification [2]. The transverse size of a strongly focused laser beam changes significantly along the beam and this results in a change of the optical intensity. Therefore, the laser pulse emits Cherenkov radiation mainly when it propagates in the vicinity of the beam waist. Reducing the waist size, on the one hand, increases the focal optical intensity but, on the other hand, decreases the radiating region. This poses a question of an optimal focusing for achieving maximum terahertz yield.

We generalize the theory of the terahertz Cherenkov radiation to the realistic case when the ultrashort laser pulse propagates as a Gaussian beam. This allows us to study the dependence of the emitted terahertz energy on the waist size of the beam for different pulse durations.

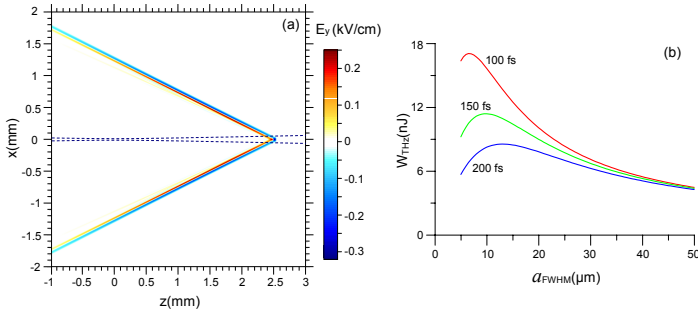


Figure 1: (a) Snapshot of the electric field $E_y(x, z, t)$. The dotted lines show the laser beam. (b) The total terahertz energy W_{THz} as a function of a_{FWHM} for different τ_{FWHM} and the fixed energy of the optical pulse $W_{opt} = 3.6 \mu$ J.

Fig. 21(a) shows the radiation pattern in LiNbO₃ from a Ti:Sapphire laser pulse with the duration $\tau_{FWHM} = 200$ fs, the waist size $a_{FWHM} = 10 \mu$ m, and the peak optical intensity 10 GW/cm^2 . The inhomogeneity of the electric field on the Cherenkov cone results from the variation of the optical intensity along the beam. Fig. 21(b) shows the total terahertz energy emitted by the pulse during its propagation from $z = -\infty$ to $z = +\infty$. For every τ_{FWHM} , there is an optimal a_{FWHM} , which increases with τ_{FWHM} .

References

- [1] Auston D.H., Appl. Phys. Lett. **43**, 713-715 (1983)
- [2] Bakunov M.I. et al, Appl. Phys. Lett. **101**, 151102 (2012)

Asymmetric terahertz Cherenkov radiation in LiNbO₃

M. I. Bakunov, E. A. Mashkovich, E. V. Svinkina*

University of Nizhny Novgorod, Nizhny Novgorod, Russia

*E-mail: elena.svinkina@gmail.com,

One of the most efficient optical-to-terahertz converters is the structure consisting of a thin (30-50 μm thick) layer of LiNbO₃ (LN) attached to a Si-prism outcoupler [1,2]. A femtosecond laser pulse propagates in the LN layer as a guided mode and produces nonlinear polarization, which emits terahertz Cherenkov radiation to the Si prism. The prism couples the radiation into free space. An inherent disadvantage of the converter is a dip in the generated terahertz spectrum originating from the destructive interference of the terahertz waves emitted to the Si prism from the LN layer directly and after reflections from the layer boundaries. We propose to remove the spectral dip by using the spatial asymmetry of the Cherenkov radiation from a moving nonlinear polarization, \mathbf{P}^{NL} , which is tilted with respect to the direction of motion [3].

The crystallographic axes in LN can be arranged in such a way that the line-like (stretched along the y axis) nonlinear polarization $\mathbf{P}^{\text{NL}}(x, \xi)$, produced by a focused-to-a-line pump laser pulse ($\xi = t - z/V$, V is the group velocity), will be almost orthogonal to the electric field \mathbf{E} (tilted with respect to the displacement \mathbf{D}) on a half of the Cherenkov wedge [Fig. 1(a)]. As a result, this half-wedge will be practically not generated [Fig. 1(b)].

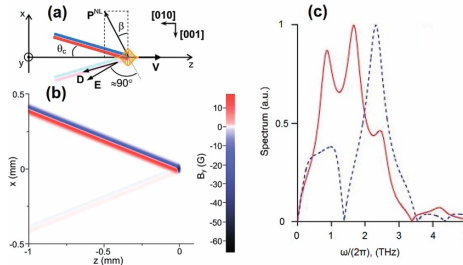


Figure 2: (a) Geometry of asymmetric Cherenkov radiation in LN. (b) Magnetic field $B_y(x, \xi)$ at $t = 0$ for laser pulse with 100 fs duration, 30 μm transverse size, and 100 GW/cm^2 peak intensity. (c) THz spectrum for the converters with asymmetric (solid) and symmetric (dashed) Cherenkov radiation [2].

We propose applying this phenomenon to the converter to concentrate the terahertz emission in the direction of the Si-prism outcoupler, thus avoiding the reflection from the LN-air boundary. This allows one to remove the dip from the spectrum [Fig. 1(c)].

References

- [1] S. B. Bodrov, M. I. Bakunov, and M. Hangyo, *J. Appl. Phys.* **104**, 093105 (2008).
- [2] M. I. Bakunov and S. B. Bodrov, *Appl Phys B* **98**, 1 (2010).
- [3] M. I. Bakunov, E. A. Mashkovich, and E. V. Svinkina, *Opt. Lett.* **39**, 6779 (2014).

Ellipticity Dependence of High-order Harmonics Generation

E. W. Larsen^{1*}, E. Lorek¹, S. Carlström¹, C. M. Heyl¹,

D. Paleček², A. L'Huillier¹, D. Zigmantas², and J. Mauritsson¹.

¹Department of Physics, Lund University, Box 118, Lund, Sweden, SE-221 00

²Department of Chemical Physics, Lund University, Box 118, Lund, Sweden, SE-221 00

*E-mail: Esben.Witting-Larsen@fysik.lth.se

High-order Harmonic Generation (HHG) is a technique routinely used in laboratories across the world to generate extreme ultraviolet (XUV) laser pulses with femtosecond or attosecond durations [1]. These pulses are commonly used to study electron dynamics in various materials such as atoms, molecules, nanoparticles, and solids. In order to obtain HHG the laser peak intensity has to exceed 10^{13} W/cm², which is normally achieved using pulsed solid state laser systems with repetition rates up to a few kHz and pulse energies above a mJ. Recent developments in fiber based amplifier systems have opened the possibility to push the repetition rate into the MHz regime using a tight focusing geometry and lower pulse energies (typically down to tens of μ J) [2-3]. The XUV pulse energies of such systems are considerably lower. However, experiments that require a modest XUV photon flux, such as coincidence detection schemes and surface science experiments with attosecond time resolution will greatly benefit from the higher repetition rate.

We study HHG at high repetition rate using a commercially available laser system [3]. The system is YB:KGW amplified laser (Pharos, Light Conversion Ltd.), which delivers pulses with a central wavelength of 1030 nm, and a duration of 170 fs operating at a repetition rate up to 700 kHz. The harmonics of this system are spectrally narrow, and are therefore well-suited for typical time-resolved spectroscopy studies in the XUV. We demonstrate the advantage of this high repetition rate long pulsed laser system by studying how ellipticity of the driving laser affects the XUV light generated by the long and short trajectories respectively [4]. Figure 3 shows the generated harmonic spectrum, when the laser is focused either before the generation medium (left panel) or in the middle of the generation medium (right panel).

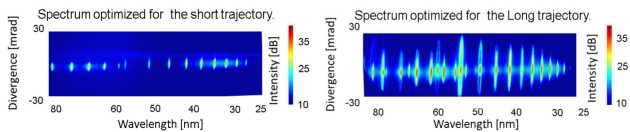


Figure 3: High harmonic spectrum recorded at 20 kHz with 170 μ J pulses.

References

- [1] P. M. Paul *et al.*, Science **292**, 1689 – 1692 (2001).
- [2] J. Boulet *et al.*, Optics Letters **34**, 1489 – 1491 (2009).
- [3] E. Lorek *et al.*, Rev. Sci. Instrum **85**, 123106-1 – 123106-5 (2014)
- [4] E. W. Larsen *et al.*, Manuscript in preparation.

Fourier-transform spectroscopy studies and deperturbation analysis of $A^1\Sigma^+$ and $b^3\Pi$ states in RbCs

A. Kruzins¹, K. Alps¹, O. Docenko¹, I. Klincare¹, M. Tamanis¹, R. Ferber¹, E.A. Pazyuk²
and A.V. Stolyarov²

¹Laser Centre, University of Latvia, Rainis blvd. 19, Riga, Latvia, LV-1586

²Department of Chemistry, Lomonosov Moscow State University, 119991 Moscow, Leninskie
gory 1/3, Russia

*E-mail: artis.kruzins@lfizmati.lv,

In heteronuclear alkali diatomic molecules containing heavy atoms, the lowest electronically excited $A^1\Sigma^+$ and $b^3\Pi$ states are strongly coupled due to the large value of spin-orbit interaction. These fully mixed states can't be examined separately and need to be considered as a single $A^1\Sigma^+ - b^3\Pi$ complex with complicated energy levels structure. $A - b$ complex can provide an efficient path to transfer ultracold molecules to their rovibrational ground state as shown in [1].

The experimental setup for these studies was the following. The $^{85}\text{Rb}^{133}\text{Cs}$ and $^{87}\text{Rb}^{133}\text{Cs}$ molecules were produced in a heat pipe oven. Excitation sources (ring dye laser, different laser diodes) were applied depending on excitation-observation scheme we were using. Backwards laser induced fluorescence (LIF) was collected with Fourier transform spectrometer Bruker IFS 125HR and recorded with the resolution of 0.03-0.05 cm^{-1} . For this studies we used two excitation-observation schemes, $A^1\Sigma^+ - b^3\Pi \leftrightarrow X^1\Sigma^+$ and $X^1\Sigma^+ \rightarrow (4)^1\Sigma^+ \rightarrow A^1\Sigma^+ - b^3\Pi$. After analysis of all spectra 8730 rovibronic term values of $A^1\Sigma^+$ and $b^3\Pi$ states were determined with an uncertainty of 0.01 cm^{-1} in the energy range [9012, 14 087] cm^{-1} covering rotational quantum numbers $J \in [6, 324]$.

Elaborated coupled-channels deperturbation analysis reproduces 97% of the experimental term values of both isotopologues with a standard deviation of 0.0036 cm^{-1} .

The reliability of the deperturbed mass-invariant potentials and spin-orbit coupling functions of the interacting $A^1\Sigma^+$ and $b^3\Pi$ states was tested by comparing calculated and experimentally observed intensity distributions for $A - b \rightarrow X$ and $(4)^1\Sigma^+ \rightarrow A - b$ transitions.

Superb accuracy of the $A - b$ complex description opened possibility to assign the observed $(5)^1\Sigma^+ \rightarrow A - b$ and $(3)^1\Pi \rightarrow A - b$ transitions.

All obtained results were published in [2].

Riga team appreciates the support from Latvian Science Council grant No. 119/2012.

References

- [1] T. Takekoshi, L. Reichsöllner, A. Schindewolf, J. M. Hutson, C. R. Le Sueur, O. Dulieu, F. Ferlaino, R. Grimm and H.C.Nägerl, Phys. Rev. Lett. **113**, 205301 (2014).
- [2] A. Kruzins, K. Alps, O. Docenko, I. Klincare, M. Tamanis, R. Ferber, E.A. Pazyuk and A.V. Stolyarov, J. Chem. Phys. **141**, 184309 (2014).

Applications of airborne optical remote sensing techniques for environmental assessment and monitoring

Dainis Jakovels

Institute for Environmental Solutions, Lidlauks, Priekuli County/Parish, LV-4101, Latvia

**E-mail: dainis.jakovels@videsinstituts.lv,*

Environmental assessment and monitoring is traditionally carried out by field surveys. The main drawbacks of field campaigns are time-consumption and limited area coverage. Airborne and satellite optical remote sensing techniques can cover large territories in very short time providing useful information to support environmental experts.

Airborne Surveillance and Environmental Monitoring System (ARSENAL) was developed by fusing six passive optical sensors operable in the spectral ranges: 280-375nm (ultraviolet, 1 spectral channel), 356-1050nm (visible-to-near infrared, up to 288 programmable spectral channels), 950-2450nm (short wave infrared, 100 spectral channels), 3000-5000nm (mid wave infrared, 64 spectral channels), 3700-4800nm (mid wave infrared, 1 spectral band with interchangeable filters), high resolution color (RGB) imaging sensor as well as laser scanner LIDAR (based on 1064nm Nd:YAG laser). The ARSENAL is capable of acquiring 454 spectral bands simultaneously, and it is installed in a twin engine aircraft BN-2T-4S Defender that can provide the collection of data at low speeds and has a maximum endurance of around eight hours.

The results from different ARSENAL campaigns will be shown to demonstrate applications of optical hyperspectral imaging and laser scanning techniques for environmental assessment.

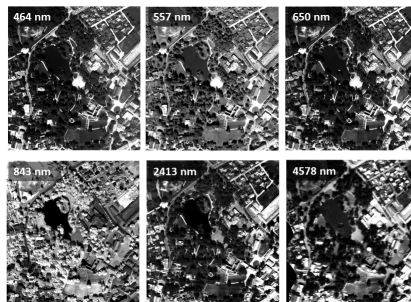


Figure 4: Cesis Castle Park: examples of several ARSENAL spectral channels. Histogram stretch is applied to show maximal contrast.

How do optical properties affect light transport in tissue, and which parameters do you need to care about in the lab?

Lise Lyngsnes Randeberg

Department of Electronics and Telecommunication, Norwegian University of Science and Technology (NTNU), Trondheim, Norway

E-mail: lise.randeberg@iet.ntnu.no,

Basic tissue properties are well known and well understood in the field of biophotonics. Optical properties are a natural first part of any curriculum in basic biophotonics. Despite this, there are important questions that are related the optical properties, which are not discussed as frequently as they should be. Questions like: how many wavelengths are needed to classify a given set of chromophores; how do the optical penetration depth affect my data analysis; and why isn't the simplest measurement always the best? This talk discusses these issues and other related questions from basic biophotonics using real life examples from tissue spectroscopy and imaging.

In addition to the basics of tissue optics, this talk will give an introduction to tissue characterization using hyperspectral imaging. This modality combines high spatial and spectral resolution in one measurement, and is flexible and adaptable to most applications. It is gaining popularity, and can be used for macro-, meso-, and macroscopic imaging, with white light, NIR or fluorescence techniques. One of the main challenges in hyperspectral imaging is the vast amount of data created. To analyze such data without throwing away interesting information requires use of both statistical tools and physics informed modeling. Hyperspectral data analysis is about finding the needle in the haystack, and preferably doing it fast. This talk will give examples of data from in vivo hyperspectral imaging with a focus on how to extract useful data and interpret them.



Figure 5: Left: Hyperspectral data cube. Two spatial dimensions are combined with a high resolution spectral dimension. A full spectrum can be retrieved from each pixel of the image. (Figure from Julio Hernandez, Norsk Eletro Optikk AS); Middle: Bruises on the forearm of two male volunteers; Right: Syntetic color image of a bruise, based on data in the NIR spectral range. See L.L. Randeberg, J. Hernandez-Palacios, Hyperspectral imaging of bruises in the SWIR spectral region, Proceedings of SPIE, Vol. 8207, 2012

Performance optimisation of biosensors based on SiON microring resonators

T. Chalyan¹, D. Gandolfi¹, R. Guider¹, L. Pasquardini², A. Samusenko³, C. Pederzoli²,
G. Pucker³, L. Pavesi¹

¹*Nanoscience Laboratory, Department of Physics, University of Trento, Via Sommarive 14,
38123 Trento, Italy*

²*LaBSSAH, Fondazione Bruno Kessler, Via Sommarive 18, 38123 Povo, Italy*

³*Centre for Materials and Microsystems, Fondazione Bruno Kessler, Via Sommarive 18,
38123 Povo, Italy*

**E-mail: tatevik.chalyan@unitn.it,*

In this work, we present a study on microring based photonic biosensors[1] for aflatoxin M1 detection, which is a major toxin for south Europe dairy industry. We measured the bulk Sensitivity (S) and Limit of Detection (LOD) as a function of the waveguide composition and dimensions. The sensing device is based on an array of four SiON microring resonators, fiber-coupled to a VCSEL (wavelength 850 nm) and a silicon photodetector and packaged into a microfluidic platform. Volumetric sensing with glucose-water solutions of various concentrations[2] was performed on 100 μm radius resonators and yields a best sensitivity of 112 nm/RIU. To link these results to the limit of detection of the sensors, we also measured the noise of our experimental readout system and deduced a best value of LOD of 1.6×10^{-6} RIU[3]. Finally, we performed sensing measurements on functionalized sensors using aflatoxin M1 solutions of various concentrations (down to 12.5nM). The functionalization is based on a wet silanization and specific DNA-aptamer binding on the chip. Reproducibility and re-usability of the sensor were also investigated by several chemical treatments. We were able to perform up to 17 measurements on a single sample without saturating the sensor. Such procedure allows multiple sequential measurements with a good endurance. This work was supported by the FP7 EU project "Symphony" (Grant agreement no: 610580).

References

- [1] AK. De Vos, I. Bartolozzi, E. Schacht, P. Bienstman and R.Baets, Optics express **15/12**, 7610-7615 (2007)
- [2] W. M. B. M. Yunus, A. B. A. Rahman, Applied optics **27/16**, 3341-3343 (1988)
- [3] <http://arxiv.org/pdf/1408.3954v1.pdf/>

Polarization-Sensitive Synchronous Fluorescence Spectroscopy of Human Basal Cell Carcinoma

Aleksandra Zhelyazkova^{1,*}, Ekaterina Borisova¹, Tsanislava Genova¹, Nikolai Penkov²,
Latchezar Avramov¹

¹*Institute of Electronics, Bulgarian Academy of Sciences, 72, Tsarigradsjo Chasussee Blvd.,
1784, Sofia, Bulgaria*

²*University Hospital "Tsaritsa Yoanna-ISUL" 8, "Byalo more" str., 1527 Sofia, Bulgaria,
1113, Sofia, Bulgaria*

**E-mail: alexandra_jivkova@abv.bg,*

As the skin is a complex multilayered and inhomogeneous organ with spatially varying optical properties, the analysis of cutaneous fluorescence spectra could be very complicated. Polarization synchronous fluorescence spectroscopy (SFS) has the potential to increase our knowledge for the origins of endogenous fluorophores, pigments content, structure alterations in normal and diseased skin. It could be applied to increase the autofluorescence diagnostic accuracy for clinical needs.

Our investigations for the autofluorescence measurements are based on ex vivo point-by-point measurements of SFS data of normal and diseased human skin samples using linear polarizer and analyzer for excitation and emission light are detected. The fluorescence excitation-emission matrix data were acquired using a commercial spectrofluorometer (FluoroLog 3, Horiba Jobin Yvon) with fiber-optic probe in steady-state regime of work using excitation wavelength in the spectral range of 280-440 nm with wavelength interval in the range of $\Delta\lambda = 0-200$ nm, and increment of 10 nm. Three different situations were evaluated and corresponding excitation-emission matrices were developed – with parallel and perpendicular positions for linear polarizer and analyzer, and without polarization of excitation and fluorescence light detected from the samples. For the experiments we used freshly excised basal cell carcinoma (BCC) tumors.

In our measurements, the most significant alterations observed were between parallel and cross-polarized fluorescence were for the short wavelength spectral region of excitation λ applied 280-360 nm, where the structural proteins excitation spectra have place. In order to further demonstrate the feasibility of this new method, studies need to be carried out to measure the fluorescence anisotropy of more skin benign and malignant lesions.

Acknowledgements:

This work is supported partially by the National Science Fund of Bulgarian Ministry of Education and Science under grant DMU-03-46/2011 and partially under grant DFNI-DO02/9/2014.

Method for registration of multispectral skin images

Roberts Kadiķis

Institute of Electronics and Computer Science,

Dzerbenes Str. 14, Riga, Latvia, LV-1006

E-mail: r.kadikis@gmail.com

A non-invasive acquisition and automatic analysis of the images of skin lesions may advance the early diagnosis of malignancies such as melanoma. A multispectral imaging is a promising technique to achieve such goal. Since the multispectral images consist of several monochrome images (bands) of same scene, it is important that same pixels in the different bands correspond to the same points in the imaged scene. This is not always the case if the bands are acquired sequentially. Therefore, a required preprocessing step, before the analysis of the multispectral images, is registration, in which all bands (sensed images) are aligned with a chosen single band (reference image).

The image registration is a widely studied topic in the image processing field, so the common classes of the registration methods are discussed. The concrete application requires fast algorithm, which is also well adjusted to the skin images. In this talk, a novel feature-based image registration method is presented. A distinctive property of the method is the possibility to use and combine different kinds of feature points. The local minima and maxima are proposed as successful features for the skin images. The method efficiently finds translation among these images by analysing all possible shifts among the feature points in the reference and sensed images. The method is expanded to also determine the rotation and scale. Further, the order of registration of the bands is analysed - how to choose the reference and sensed images for a successful registration of all bands.

A dataset of 60 multispectral images (each containing 51 spectral bands) was manually registered. Then the dataset was used to test the proposed method and several other common methods: area based methods with sliding patches; feature based methods with SURF and SIFT descriptors. Test results are depicted in the table 1, where the second column shows how many of the 3000 spectral bands were registered correctly.

Table 1: Comparison of several image registration methods.

Method	Correctly registered
Sliding patches of size 50×50 pixels	80.0%
Sliding patches with SSC	58.1%
Feature point matching using SURF descriptor	74.7%
Feature point matching using ORB descriptor	64.9%
Proposed method	84.5%

In conclusion, the proposed method is suitable for the concrete application. It performs relatively well on the dataset and is computationally efficient. A drawback of the method is its inability to detect nonlinear or local transformations among sensed and reference images. However, the ability to use different types of feature points makes the proposed method potentially applicable to other registration applications, in addition to the registration of multispectral skin images.

Estimation of rosacea treatment effectiveness by RGB imaging

Inga Saknite^{1*}, Aleksejs Zavorins², Janis Spigulis¹, Janis Kisis²

¹*Biophotonics Laboratory, Institute of Atomic Physics and Spectroscopy, University of Latvia, Raina Blvd 19, Riga, LV-1586, Latvia*

²*Department of Infectology and Dermatology, Riga Stradins University, Linezera Str 3, Riga, LV-1006, Latvia*

**E-mail: inga.saknite@lu.lv,*

Rosacea is a chronic skin disorder that gives facial skin (mostly cheeks, chin, nose and forehead) red color, visibly seen blood vessels, and, if untreated, can develop to bumps and pimples on skin surface [1]. RGB imaging is a simple tool that can be used to evaluate the redness of skin as there is a strong absorption of skin chromophore hemoglobin in the spectral range of 500-600 nm, which corresponds to the green channel of an RGB camera. Erythema index is usually used as a quantitative estimation of the redness, and it is usually expressed as a difference between red and green spectral channels [2]. Different commercially available devices are used in clinics (e.g. Mexameter) that calculate erythema index as a point measurement [3].

This study focuses on erythema index estimation by using an RGB imaging device Skimager, developed at the Biophotonics Laboratory, Institute of Atomic Physics and Spectroscopy. Skimager acquires red, green and blue channel images at different illuminations: white, 450 nm, 540 nm, 660 nm, and 940 nm LEDs. Skimager acquires images that are used to calculate mean erythema index from a skin area of around 3 x 3 cm, instead of a point measurement.

100 rosacea patients participated in a study: for a month every day, they were using a lotion that is thought to reduce rosacea symptoms. Half of the patients were in a control group (using a moisturizing cream) and half of them were using the rosacea treatment lotion, without knowing which cream they are using. Two measurements have been acquired: at the beginning of the study and one month after. Measurements were done by Mexameter and Skimager at 5 different parts of facial skin: forehead, left cheek, right cheek, left part of a nose, right part of a nose. Results of both devices were compared, and effectiveness of the rosacea treatment lotion is estimated and discussed.

Acknowledgements

This study was supported by the European Social Fund project "Innovative biomedical image acquisition and processing technologies", grant no. 2013/0009/1DP/1.1.1.2.0/13/APIA/VIAA/014.

References

- [1] <http://www.rosacea.org/patients/allaboutrosacea.php>
- [2] Jakovels, D., Kuzmina, I., Berzina, A., Valeine, L., Spigulis, J., Noncontact monitoring of vascular lesion phototherapy efficiency by RGB multispectral imaging. *Journal of Biomedical Optics*, 18(12), 126019-126019 (2013)
- [3] Clarys, P., Alewaeters, K., Lambrecht, R., Barel, A. O., Skin color measurements: comparison between three instruments: the Chromameter, the DermaSpectrometer and the Mexameter. *Skin research and Technology*, 6(4), 230-238 (2000)

Spectral reflectance estimation with an optical non contact device for skin assessment

Jacob Bauer^{1,2}, Ville Heikkinen², Janis Spigulis¹

¹ *Biophotonics Labrotory, Institute of Atomic Physics and Spectroscopy, University of Latvia, 19 Rainis Blvd., Riga, LV-1586, Latvia*

² *CIMET - School of Computing, University of eastern Finland, P.O.Box 111, FI-80101 Joensuu, Finland*

*E-mail: Jacob.Bauer@me.com,

Skin chromophores like hemoglobin and bilirubin provide useful information about the health status of skin. In a proof of concept study a low cost hand held imaging device has been developed[1]. The SkImager is based on a multi illumination LED ring and a CMOS sensor (see figure 21). Different absorbance properties of various skin chromophores are being used to study their concentration[1]. The main goal of this research is to explore the quality of this working prototype for spectral estimations. The accuracy of this estimation is determined by the number of spectral channels and the used spectral estimation method. Spectral estimation can be performed with several well known estimation methods like the Wiener estimation or the linear least squares fitting and have been optimized for spectral estimation of skin samples [2]. A Suitable spectral estimation method to obtain chromophore concentration maps shall be developed and analyzed. The results obtained shall be compared to the existing chromophore map workflow used in the SkImager.

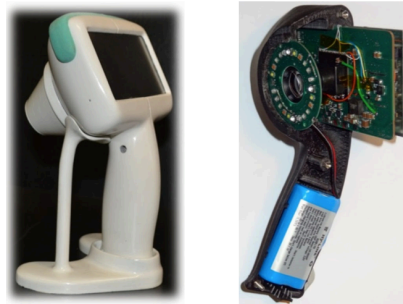


Figure 6: SkImager optical non contact Device with LED Ring (5 different Illuminations) and CMOS Sensor[1]

References

- [1] Spigulis Janis and Rubins, Uldis and Kviesis-Kipge, Edgars and Rubenis, Oskars, SkImager: a concept device for in-vivo skin assessment by multimodal imaging, *Proceedings of the Estonian Academy of Sciences*, **63**, 213-220 (2014)
- [2] Chen, Shuo and Liu, Quan, Modified Wiener estimation of diffuse reflectance spectra from RGB values by the synthesis of new colors for tissue measurements, *Journal of biomedical optics* **17**, 0305011-0305013 (2012)

Development of a Fiber-top Controlled Adaptable Stiffness Needle

Steven Beekmans^{1,*}, John van den Dobbelsteen², Davide Iannuzzi¹

¹*Biophotonics and Medical Imaging, VU Laserlab, VU University Amsterdam*

²*Department of BioMechanical Engineering, Delft University of Technology*

*E-mail: s.v.beekmans@vu.nl

Each year, in the Netherlands alone, more than 50.000 percutaneous procedures are performed for treatment or for removal of tissue from possibly diseased organs, of which 15.000 return non-diagnostic due to erroneous needle targeting. In this study, we aim to facilitate needle targeting by combining two unique, mechanical instruments: a needle with adaptable stiffness and a probe that can identify tissues via real-time measurements of their mechanical properties. Besides facilitating needle targeting, integration of these tools in one instrument enables a new kind of on-line optical biopsy on the basis of mechanical properties of tissue at the tip of a needle.

The needle will consist of a flexible shaft with a fully actuated tip based on a miniature cable-driven steerable mechanism previously developed [1]. The stiffness of both the shaft and the needle steerable mechanism can be adapted by adjusting the tensioning of the cables incorporated in the needle. An all-optical, highly sensitive, interferometric sensor is mounted at the tip of the needle. When the needle encounters the interface between two layers of tissue a fiber-based nanoindenter inside the needle is extended and used to accurately measure the stiffness of the tissue that is about to be perforated. This indenter consists of a micromachined cantilever which is fabricated on top of an optical fiber [2]. Upon contact with the tissue the cantilever bends to a degree determined by the stiffness of the sample. By coupling light from the opposite end of the optical fiber, the cantilever position is assessed. Besides its diagnostic value, the mechanical information of the tissue is fed back to the needle and used for active manipulation of the needle's stiffness.

Indentation experiments have been performed on gel samples by mechanically actuating the fiber-based sensor at the tip of a steerable needle. Furthermore, indentation experiments on ex vivo mouse brain tissue have been carried out in order to validate the sensor principle. To gain a measure for tissue stiffness, the load-indentation data has been analyzed by the Oliver and Pharr as well as the Hertz model. The resulting Young's Modulus for brain tissue was found between 1-10 kPa, depending on the functional region of the brain. In conclusion, we have shown to be able to actuate the sensor at the distal end of the needle using a remote indentation system. Furthermore, we have proven to be able to quantify the mechanical properties, in terms of Young's Modulus, of soft tissue by means of indentation, with results comparable to literature. These results provide valuable insights for the continuation of this study.

References

- [1] C. Fan, H. Clogenson, P. Breedveld, J. J. van den Dobbelsteen and J. Dankelman, *J. Med. Devices*, **6**, no 2 (2012)
- [2] D. Iannuzzi, S. Deladi, V. J. Gadgil, R. G. P. Sanders, H. Schreuders and M. C. Elwenspoek, *Appl. Phys. Lett.*, **88**,053501 (2006)

Nitrogen Vacancy Centers in Diamonds for Sensing and Quantum Information

Dr. Florian Gahbauer

Laser Centre, University of Latvia

E-mail: florian.gahbauer@lu.lv,

Among the many different types of defects found in diamond crystals, nitrogen-vacancy (NV) centers have particularly interesting properties that make them suitable for applications in sensing, particularly magnetic field sensing, and quantum information. These properties are based on the fact that the NV centre has a triplet ground state, with three possible values for the projection m_s of the spin on the quantization axis: 0 and ± 1 . This ground state can be pumped into the $m_s = 0$ component by irradiating the NV centre with green light for a short time. Moreover, the polarization state can be determined from the fluorescence intensity. The $m_s = \pm 1$ components are degenerate at zero magnetic field and have a zero-field splitting of 2.87 GHz with respect to the $m_s = 0$ component, which increases by 5.6 MHz/G as the magnetic field is increased. As a result, the ground state spin state can be manipulated by microwave fields and interacts with magnetic fields from the environment and nearby spins. Controlled manipulations of these interactions lead to interesting applications in magnetic field sensing and quantum information. We will give an overview of the physics of NV centers and discuss their applications.

Temperature dependence of the local structure of Y_2O_3 from EXAFS analysis using evolutionary algorithm method

Inga Jonane*, Janis Timoshenko

Institute of Solid State Physics, Kengaraga 8, Riga, Latvia, LV-1063

**E-mail: ingajonaane@gmail.com*

Yttrium sesquioxide (Y_2O_3) is an important optical material. Doped Y_2O_3 , for instance, attracts much attention as a phosphor for optical display and lighting applications [1, 2]. Y_2O_3 is also used in rare-earth ion doped lasers [3].

Crystalline Y_2O_3 has body-centered cubic structure (space group $Ia\bar{3}$), with the unit cell consisting of 80 atoms [4]. Due to this complicated structure, the understanding of properties of Y_2O_3 at the atomic scale is a challenging task, which should be addressed using modern experimental and theoretical approaches.

We have investigated the local structure of Y_2O_3 using the extended X-ray absorption fine structure (EXAFS) spectroscopy. EXAFS data, acquired at the Y K-edge, were interpreted using the novel reverse Monte Carlo and evolutionary algorithm (RMC/EA) approach [5]. This method allows one to find via iterative random process a 3D structure model of the investigated material that gives the best agreement between experimental and theoretically calculated EXAFS data (Fig. 21).

RMC/EA-EXAFS approach allowed us to follow the evolution of local structure of crystalline Y_2O_3 upon temperature increase from 300 K up to 1300 K and to analyze the influence of structural and thermal disorder in crystalline and nanocrystalline Y_2O_3 .

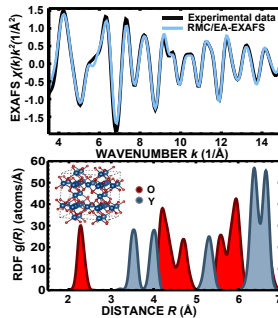


Figure 7: Unit cell of crystalline Y_2O_3 and the results of RMC/EA calculations for crystalline Y_2O_3 at room temperature: experimental and calculated Y K-edge EXAFS spectra, and the radial distribution function (RDF) around Y atom.

References

- [1] T. Igarashi, M. Ihara, T. Kusunoki, et al., Appl. Phys. Lett. **76** 1549 (2000)
- [2] Z. Qi, C. Shi, W. Zhang, et al., Appl. Phys. Lett. **81**, 2857 (2002)
- [3] L. Jianren, L. Junhua, et al., Jap. J. Appl. Phys. **40**, L1277 (2001)
- [4] F. Hanic, M. Hartmanova, G.G. Knab, et al., Acta Cryst. B **40**, 76 (1984)
- [5] J. Timoshenko, A. Kuzmin, J. Purans, J. Phys.: Condens. Matter **26**, 055401 (2014)

Impact of oxygen related defects on the properties of up-conversion luminescence of $\text{NaLaF}_4\text{:Er}^{3+}$ material

Guna Doke^{1*}, Guna Krieke², Jurgis Grube¹, Anatolijs Sarakovskis¹, Maris Springis¹

¹*Institute of Solid State Physics, Kengaraga 8, Riga, Latvia, LV-1063*

²*Institute of General Chemical Engineering, Riga Technical University, Paula Valdena 3, LV-1048*

**E-mail: guna.doke@gmail.com,*

Fluorides and complex fluorides are considered to be very attractive host materials for optically active trivalent rare-earth (RE) ions. These materials have been used for decades to study properties and possible applications of up-conversion (UC) luminescence. One of the most significant problem of fluoride materials is emerging of oxygen-related defects as result of synthesis. In our laboratory in-depth studies of $\text{NaLaF}_4\text{:RE}$, including creation of different methods of synthesis, have been carried out for several years.

In this work, two $\text{NaLaF}_4\text{:Er}^{3+}$ samples with Er^{3+} concentration of 2.0 mol% were synthesized in different atmospheres (air, fluorine).

For both samples luminescence, excitation spectra, decay kinetics were measured by using excitation at ultraviolet, visible and infrared (IR) spectral region. In addition measurements of IR absorption and structural studies were performed. Analysis of the results showed that synthesis in air atmosphere stimulate formation of oxygen-related defects and the presence of these defects significantly impact intensity of UC luminescence, the green/red luminescence band ratio and UC mechanisms.

Azobenzene containing molecular glass as an optical recording material

Krista Klismeta^{*}, Janis Teteris

Institute of Solid State Physics, Kengaraga 8, Riga, Latvia, LV-1063

^{*}E-mail: k.klismeta@gmail.com

Under influence of light azo compounds experience *trans-cis* isomerisation process [1]. As a result, the moieties may align relative to the electric field vector of light. This leads to anisotropy in the material (observed as dichroism and birefringence) [2] and also macroscopic movement of mass could occur on the surface of the film [3]. The orientation process is easier in low molecular weight organic glasses containing the azo chromophore because the geometry of the moiety prevents crystallization.

In this work photoinduced processes in azobenzene containing low-molecular weight organic glass K-RJ-8 were experimentally studied. The compound was synthesized in Riga Technical University. Photoinduced dichroism and birefringence in the visible spectrum was studied. To induce the mass motion holographic recording using different polarization states of the recording beams was done. During the recording of the surface relief gratings diffraction efficiency was measured, the resulting formation was measured by atomic force microscopy.

References

- [1] Yager, K. G. et al., *Smart light-responsive materials* (Wiley, Hoboken, New Jersey 2009)
- [2] Nikolova, L. et al., *Polarization Holography* (Cambridge University Press, New York 2009)
- [3] Rochon, P. et al., *Appl. Phys. Lett.* **66**, 136 - 138 (1995)

Amplified spontaneous emission of DCM derivative in PVK thin film.

M. Narels^{1,*}, A. Vembris¹

¹*Institute of Solid State Physics, Kengaraga 8, Riga, Latvia, LV-1063*

*E-mail: martins.nar@gmail.com

Organic materials are promising candidates for wide variety of modern applications, one of such is optically pumped organic solid-state lasers. This application requires materials with high light amplification coefficient and low threshold values, which in most of the cases in organic systems is limited by crystallization of dye molecules and formation of their aggregates. Compounds with reduced crystallization would be beneficial in organic laser systems due to higher possible dopant concentrations.

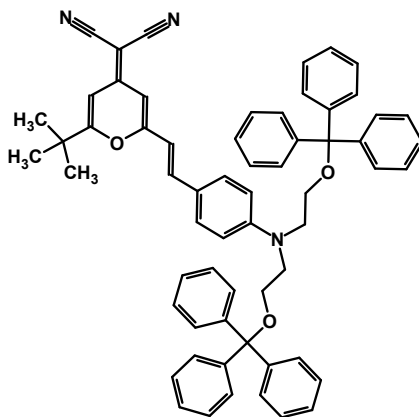


Figure 8: Chemical structure of the DCM derivative.

In the work we investigate thin films with newly synthesized material 2-(2-(4-(bis(2-(trityloxy)ethyl)amino)styryl)-6-tert-butyl-4H-pyran-4-ylidene) malononitrile (derivative of widely-known laser dye DCM) doped in PVK polymer matrix. Thin-films were made with various dopant concentrations (0.1 wt% - 100 wt%) and thickness approximately 300 nm. For these films photoluminescence spectrum and amplified spontaneous emission measurements were performed using 405 nm diode laser and Nd:YAG pulse laser with wavelength 532 nm, respectively. Results will be discussed.

Photoluminescence in Er^{3+} -doped $0.4\text{Na}_{0.5}\text{Bi}_{0.5}\text{TiO}_3-(0.6-x)\text{SrTiO}_3-x\text{PbTiO}_3$ solid solutions

Marija Dunce*, Eriks Birks, Anatolijs Sarakovskis, Maija Antonova, Andris Sternberg
Institute of Solid State Physics, Kengaraga 8, Riga, Latvia, LV-1063

*E-mail: marija.dunce@cfi.lv.lv,

$\text{Na}_{1/2}\text{Bi}_{1/2}\text{TiO}_3$ -containing solid solutions attract interest mostly as an alternative for nowadays widely used ferroelectrics with high lead content, use of which is gradually limited due to environmental considerations. Additional interest to preparing and studying such compositions is connected with a possibility to obtain relaxor ferroelectrics, which are a hot topic in physics of ferroelectrics, as their properties are not completely understood, but are very attractive for different applications.

A transfer from relaxor to normal ferroelectric state, passing various sequential states, characteristic for relaxor ferroelectrics, was found in $0.4\text{Na}_{1/2}\text{Bi}_{1/2}\text{TiO}_3-(0.6-x)\text{SrTiO}_3-x\text{PbTiO}_3$ solid solutions, if Pb content is increased [1]. X-ray diffraction measurements revealed coexistence of phases with tetragonal and cubic symmetries in the concentration and temperature region, where relaxor properties were observed. In order to gain insight into differences of local environment in these solid solutions, comparing ferroelectric and relaxor state, photoluminescence of Er^{3+} -doped $0.4\text{Na}_{1/2}\text{Bi}_{1/2}\text{TiO}_3-(0.6-x)\text{SrTiO}_3-x\text{PbTiO}_3$ is studied in the present work.

Upon excitation at 490 nm ($^4\text{I}_{15/2} \rightarrow ^4\text{F}_{7/2}$), traditional photoluminescence bands in the green ($^4\text{S}_{3/2} \rightarrow ^4\text{I}_{15/2}$) and red ($^4\text{F}_{9/2} \rightarrow ^4\text{I}_{15/2}$) parts of the spectrum are observed. The same luminescence bands are also excited at 980 nm ($^4\text{I}_{15/2} \rightarrow ^4\text{I}_{11/2} \rightarrow ^4\text{F}_{7/2}$) corresponding to upconversion luminescence processes in the material.

Luminescence spectra and decay kinetics of the materials are studied at different temperatures with respect to the composition factor. The results obtained for relaxor and ferroelectric states are mutually analyzed and the impact of ferroelectric ordering on the luminescence properties is discussed.

References

[1] M. Dunce, M. Antonova, E. Birks, M. Kundzinsh, A. Sternberg, *Integrated Ferroelectrics* **108**, 125-133 (2009)

Modeling absorption spectrum of skin in the near-infrared spectral range by Monte Carlo simulations

Gatis Tunens, Inga Saknīte, Janis Spigulis

Biophotonics Laboratory, Institute of Atomic Physics and Spectroscopy, Raina Blvd 19, Riga, LV-1586, Latvia

This research looks at the Monte Carlo simulations as a tool to model near-infrared absorption spectra of human skin for a better understanding of its optical properties in the near-infrared spectral range. This would be helpful in analyzing changes in skin moisture by optical methods. This study consists of doing Monte Carlo simulations for known spectra of different molecules inside the human skin (e.g. water (see Figure 21), carbohydrates).

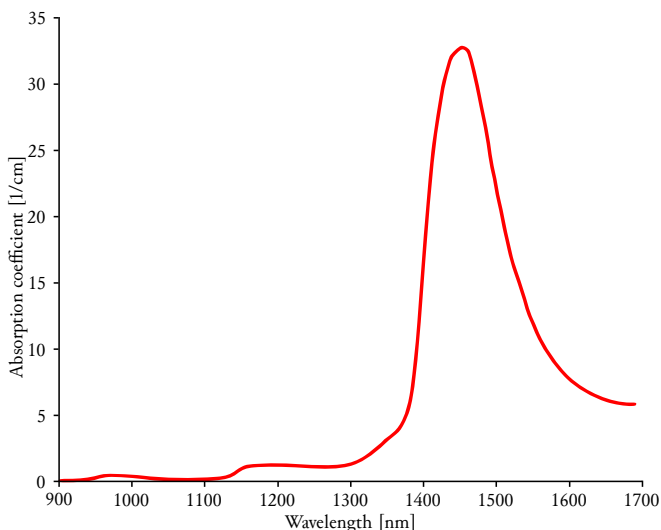


Figure 9: Absorption spectrum of water in the spectral range of 900 - 1700 nm^[1].

The results of these simulations are then used to compare experimental data of absorption spectra of human skin to obtain relative concentration values of the absorbing molecules in skin. This will be accomplished by using reverse Monte Carlo simulations. The results of this research show a potential to be used as a tool for obtaining information about skin moisture level by understanding the absorption and scattering properties of skin in the near-infrared spectral range.

References

- [1] <http://omlc.org/spectra/water/data/>

Snapshot mapping of skin chromophores at triple-wavelength illumination

Ilze Oshina^{1,*}, Janis Spigulis²

¹*Biophotonics Laboratory, Institute of Atomic Physics and Spectroscopy, University of Latvia,
Rainis blvd. 19, Riga, LV-1586, Latvia*

^{*}*E-mail: osina.ilze@gmail.com,*

Fast and reliable imaging of skin has a potential in clinical applications. It could be provided by single snapshot tri-chromatic spectral imaging.

Monochromatic spectral images at the illumination wavelengths 473nm, 532nm and 659nm were extracted from single RGB image data set by separate registration of the R, G and B output values from each image pixel[1]. First we map spectral reflectance k_λ at three chosen wavelengths. Spectral reflectance is the ratio between the intensity of radiation reflected from the target at the specified wavelength $I(\lambda)$ and the intensity of radiation, reflected at this wavelength from a non-absorbing white reference $I_o(\lambda)$.

Second we convert these three monochromatic images into distribution maps of skin oxy-hemoglobin, deoxy-hemoglobin and melanin. To do that we use system of 3 equations based on the Beer-Lambert law [2,3]:

$$\begin{cases} c_a \cdot \varepsilon_a(\lambda_1) + c_b \cdot \varepsilon_b(\lambda_1) + c_c \cdot \varepsilon_c(\lambda_1) = -\frac{\ln k_1}{l_1} \\ c_a \cdot \varepsilon_a(\lambda_2) + c_b \cdot \varepsilon_b(\lambda_2) + c_c \cdot \varepsilon_c(\lambda_2) = -\frac{\ln k_2}{l_2} \\ c_a \cdot \varepsilon_a(\lambda_3) + c_b \cdot \varepsilon_b(\lambda_3) + c_c \cdot \varepsilon_c(\lambda_3) = -\frac{\ln k_3}{l_3} \end{cases} \quad (1)$$

c_i - relative concentration of the chromophore (a - oxy-hemoglobin, b - deoxy-hemoglobin, c - melanin), $\varepsilon_i(\lambda_j)$ - extinction coefficient of the specified chromophore ($i = a, b, c$) at j -wavelength ($1 = 473 \text{ nm}$, $2 = 532 \text{ nm}$, $3 = 659 \text{ nm}$), k_j - spectral reflectance and l_j - wavelength-dependent mean optical path length ($j = 1, 2, 3$).

As a result, pigmented malformation area showed increased melanin content, while vascular pathologies showed notable changes in oxy- and deoxy-hemoglobin content.

This method can be used in digital RGB cameras for fast and reliable express-diagnostics of skin by adding an adjusted poly-chromatic illumination source and appropriate software.

This work was supported by the European Regional Development Fund project "Innovative technologies for optical skin diagnostics" (#2014/0041/2DP/2.1.1.1.0/14/APIA/VIAA/015) and by the Latvian National research program SOPHIS under the grant agreement # 10-4/VPP-4/11.

References

- [1] J.Spigulis, L.Elste. "Single-snapshot RGB multispectral imaging at fixed wavelengths: proof of concept." Proc.SPIE, 8937, 89370L (2014).
- [2] D. Jakovels, J. Spigulis, "2-D mapping of skin chromophores in the spectral range 500-700 nm", J. Biophoton. 3, 125-129 (2010).
- [3] I. Kuzmina, I. Diebele, D. Jakovels, J. Spigulis, L. Valeine, J. Kapostinsh, A. Berzina, "Towards noncontact skin melanoma selection by multispectral imaging analysis", J. Biomed. Opt. 16, 060502 (2011).

Numerical calculation of DOS in nanograting layers using method of auxiliary sources

Vitali Ghoghoberidze^{1,*}, Sergey Petrosyan², Mikheil Mebonia²,
D. Kakulia¹, and A. Tavkhelidze²

¹*Ivane Javakhishvili Tbilisi State University, 3 Ilia chavchavadze ave., Tbilisi, Georgia*

²*Ilia State University, Kakutsa Chelokashvili Ave 3/5, Tbilisi 0162, Georgia*

*E-mail: vitali.gogoberidze@hotmail.com,

New materials are required for a new generation of energy converters and coolers. Nanostructuring allows changing material properties so that they satisfy the requirements of a particular energy conversion device. Modern solar cells comprised of semiconductor layers. Photons absorbed in these layers generate an electron hole pair. The $p - n$ junction which is formed by the thin layers separates electrons and holes and forces electrons to run through the load to perform useful work. Conversion efficiency and other parameters strongly depend on charge carrier (electron and hole) mobility in thin layers [1]. Nanograting fabricated on the surface of thin layer increases carrier mobility and improves the characteristics of solar cells [2]. Nanograting changes material properties. These changes are fully determined by the density of quantum states $\rho(E)$. Changes in itself can be described by introducing geometry factor G such that $\rho(E) = \rho_0(E)/G$ where, $\rho_0(E)$ is density of states in plain layer[3]. To calculate G Schrodinger time-independent equation should be solved in Nanograting geometry. It was one of the goals of the work to solve this problem using numerical methods. There is a full mathematical analogy between quantum billiards and electromagnetic resonators. Therefore, it is reasonable to use the Method of Auxiliary Sources (MAS) for quantum billiard calculation, as it is most efficient numerical approach for solving eigen value problems. It was one of the goals of the project to solve this problem using digital methods. Method of Auxiliary Sources (MAS) has been proposed by Georgian mathematician V. Kupradze [4]. Method was adopted by Georgian scientists for solving eigen value problems related to wave guides with arbitrary cross-section [5, 6]. In the MAS for EM boundary value problems are solved numerically by representing the electromagnetic fields in each domain of the structure by a finite linear combination of fundamental solutions of the relevant field equations, corresponding to sources situated at some distance from the boundaries of each domain. The "auxiliary sources" producing these solutions are chosen to be elementary currents/charges located on fictitious auxiliary surface, usually conforming to the actual surface of the structure. The method only requires points on the auxiliary and actual surfaces, without resorting to the detailed mesh structures as required by other methods. Finally the problem is reduced to linear system of algebraic equations. Solution of which are coefficients of the decomposition. Coefficients should be obtained by solving of the mentioned linear system where one of the coefficients is fixed. It means that the field inside area of interest becomes non-trivial only when the main parameter of the problem is near to eigenvalues and we can easily observe the forming of eigenfunctions. Intensity of the field reaches maximum on eigenvalues. We wrote our program in Fortran code. it contains two files. First part generated digital array analogous to the boundary conditions of quantum billiard and creates 100 auxiliary sources on its basis. The second part of the program sums radiation from the sources and finds wave vector value. In the case of project success, we will be able to change Si properties in such a way that high efficiency solar cells can be prepared from Si material Using interference lithography we

fabricate (NG) on the surface of thin layers to change their electronic properties. Using these techniques, gratings with 10-nm and even sub-10 nm pitch were fabricated.

References

- [1] N. Peranio, M. Winkler, D. Bessas, Z. Aabdin, J. König, H. Böttner, R.P. Hermann, O. Eibl, Journal of Alloys and Compounds, 521, 25, pp. 163–173 (2012)
- [2] A. Tavkhelidze, V. Svanidze, International Journal of Nanoscience, Vol. 7, No. 6, pp. 333-338 (2008)
- [3] A. Tavkhelidze, J. Appl. Phys. 108, 044313 (2010)
- [4] V. Kupradze, in Success of Mathematical Sciences, vol. 22, Moscow, pp. 59-107 (1967)
- [5] G. N. Ghvedashvili, K. N. Tavzarashvili, D. G. Kakulia, R. S. Zaridze, Telecommunication and Radio engineering. Volume 66, Issue 14, pp. 1265-1272 (2007)
- [6] K. Tavzarashvili, Ch. Hafner, Cui Xudong, Ruediger Vahldieck, D. Kakulia, G. Ghvedashvili, D. Karkashadze, Vol. 4, #3, pp. 667-674 (2007)

Luminescence studies of europium and coactivator doped oxyfluoride glasses and glass ceramics

Meldra Kemere¹, Janis Sperga¹, Uldis Rogulis¹, Jurgis Grube¹, Guna Krieke^{1,2},
Edgars Elsts¹

¹*Institute of Solid State Physics, University of Latvia, Kengaraga 8, Riga, Latvia, LV-1063*

²*Institute of General Chemical Engineering, Riga Technical University, Azenes 14/24, Riga, Latvia, LV-1048*

**E-mail: m.meldra@inbox.lv,*

Oxyfluoride glasses and glass ceramics doped with Eu ions are considered as prospective white light luminophores which can be used in the WLEDs[1]. In this research, we have investigated the influence of two ions (Eu and other RE ion) on the luminescence spectra of the samples using different excitation wavelength. The goal of our research is to find a sample with the highest CRI (color rendering index) value.

Transparent oxyfluoride glasses co-doped with Eu^{3+} and another RE ion: Tb^{3+} , Dy^{3+} , Sm^{3+} , Ho^{3+} , and Er^{3+} (concentration of approx. 1 mol %) have been produced. By a controlled heating of the glass samples at certain crystallization temperatures we obtained glass ceramics in which CaF_2 crystallites can be observed.

Eu^{3+} provides an effective luminescence in the red part of the spectrum while other dopants show a luminescence concentrated around the green and yellow part of the spectrum. The luminescence intensity of the above mentioned coactivators is comparable to the luminescence intensity of Eu^{3+} . However, the intensity ratio of europium and coactivator luminescence strongly depends on the excitation wavelength. Using the data acquired by the luminescence spectra we calculated CIE color coordinates and CRI index values.

References

[1] I. Brice, U. Rogulis, E. Elsts, J.Grube, Latv. J. of Phys. Tech. Sci **Nr. (I)**, 44 (2012)

HD 50975: a yellow supergiant in a spectroscopic binary system

Edite Paule*, Laimons Začs

Laser Center, University of Latvia, Raiņa bulvāris 19, Rīga, Latvia, LV-1586

**E-mail: edite.paule@gmail.com*

Astronomical spectroscopy is a field of astronomy that uses spectral instruments as a tool to acquire and analyze optical spectra of electromagnetic radiation from hot celestial objects. By studying positions, intensities and shapes of lines in obtained spectra one can deduce such properties of stars as their chemical composition, mass, luminosity, temperature, also distance to observer and relative motion of distant stars. This can help one to understand the evolution of celestial objects and the Universe itself.

HD 50975 is a recently discovered spectroscopic binary system that consists of F8 Ib super-giant and an early type star of type B2. This system is studied with a goal to estimate fundamental parameters of both components of binary system [1] and is interesting since in recent studies [2, 3] a self-consistent model of a yellow super-giant star as a possible progenitor of a supernova was proposed. Thus a comprehensive analysis of such binary systems can advance our understanding of supernova evolution.

In this study we focus on the analysis of several lines in the spectrum of HD 50975 in the range from 6000 Å up to 10000 Å, which are associated with the presence of gadolinium (Gd), europium (Eu) and dysprosium (Dy) elements (see Fig. 21). These elements are products of so called r-processes. Recent analysis has shown that the mean europium abundance in the atmosphere of HD 50975 is relatively higher than it is in the Sun atmosphere [1], which is unusual. In this study we are using atmosphere model method to confirm and explain this result.

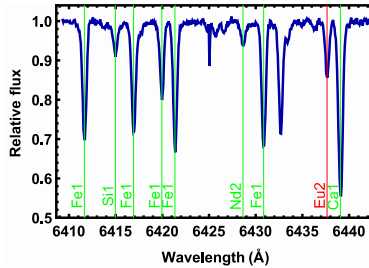


Figure 10: Spectral line, associated with Eu isotope in a fragment of optical spectrum of HD50975 binary system.

References

- [1] Sperauskas, J., Začs, L., Raudeliūnas, S., Musaev, F., Puzin, V. *Astronomy and Astrophysics*, **570**, A3 (2014)
- [2] Bersten, M. C., Benvenuto, O. G., Nomoto, K. I., Ergon, M., Folatelli, G., Sollerman, J., et al. *The Astrophysical Journal*, **757**, 31 (2012)
- [3] Benvenuto, O. G., Bersten, M. C., Nomoto, K. I. *The Astrophysical Journal*, **762**, 74 (2013)

GNSS – More Than A Simple Tool For Navigation

Inga Brice*, Janis Alnis

Institute of Atomic Physics and Spectroscopy, Skunu iela 4, Riga, Latvia

University of Latvia, Raina Bulvaris 19, Riga, Latvia, LV-1586

**E-mail: inga02@inbox.lv,*

GNSS (Global Navigation Satellite System) is free and available to anyone with a GNSS receiver. The location, time of day or weather do not matter the one necessary requirement is a signal from 4 or more satellites. Most GNSS receivers rely on both the more known GPS and on more recent GLONASS for a more accurate location due to more satellites being visible.

The information obtained from satellites can be used for more than just calculating the location of the GNSS receiver but also as a source of accurate time. Each satellite transmits the time and the location and to transmit a precise time it carries several Rb or Cs atomic standards on board. The time can be used as a reference clock to discipline a Rb clock on Earth.

Rb frequency standard is the most inexpensive, compact, and widely used type of atomic clock but it is less accurate than a Cs atomic clock and might drift by approximately 10^{-11} per month [1]. Satellites can be used for long term stabilization of the oscillator in the Rb standard. This takes approximately 10000-100000 s to assure a long term stability. We continue to gather data and keep monitoring the operation of both the Rb standard and the GNSS.

Why would one need a more accurate Rb clock? The Rb frequency standard is a likely weak point for creating optical frequency standard using femtosecond frequency comb to create an even better and accurate frequency standard and even more precise optical standard clock.

References

[1] J. C. Camparo, *A Partial Analysis of Drift in the Rubidium Gas Cell Atomic Frequency Standard*, Proc. 18th Annu. Precise Time and Time Interval Applications Planning Meeting, pp.565 -588 (1986)

Magnetic field imaging using nitrogen vacancy (NV) centres in a diamond lattice

Andris Berzins¹, Kaspars Erglis², Ruvin Ferber¹, Florian Gahbauer¹, Andrejs Jarmola^{1,3}, Sean Lourette³

¹*Laser Centre, University of Latvia, Zellu St. 8, Riga, Latvia, LV-1002*

²*Laboratory of Magnetic Soft Matter, University of Latvia, Zellu St. 8, Riga, Latvia, LV-1002*

³*Department of Physics, University of California, Berkeley, USA, CA 94720-7300*

**E-mail: andris.beerzinsh@gmail.com,*

Magnetic field imaging and magnetic field detection has a wide range of possible applications, that can be used in many disciplines such as physics, biology and chemistry. Possible applications include data storage and medicine. The specific features of NV centers allow them to be used to image both magnitude and direction of magnetic field distributions with very high spatial resolution while maintaining relatively good magnetic field sensitivity. Moreover, diamond is mechanically resistant and its thermal conductivity is very high. Also NV centres in diamond can be implanted at different depths and with different concentrations, which allows flexible solutions for different problems. As a result, NV centres in diamond is one of the hot topics in physics during the last years.

In our studies we focused on imaging small magnetic particles (with diameters of 5 μm , 2 μm and 500 nm) using a diamond sample with NV centres localized in 10 nm thick layer located about 100 nm below one of the crystal surfaces. Experiment was carried out in following way: we applied external magnetic field in direction that makes equal angles with respect to all four possible orientations of the NV centres in the diamond lattice. This allowed us to obtain optically detected magnetic resonance (ODMR). The local magnetic fields of the particles caused position-dependent frequency shifts in the ODMR, which indicated the strength of the magnetic field. An example of the images we have obtained is shown in Fig. 21.

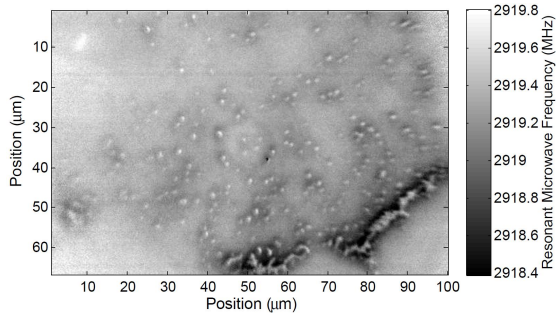


Figure 11: Position (x and y axes) and resonance frequency (color scale) of magnetic particles of size 500 nm.

High resolution laser spectroscopy and potential construction of the low-lying $^1\Pi$ electronic states in KCs and RbCs molecules

Inese Birzniece*, Olga Nikolayeva, Maris Tamanis, and Ruvin Ferber

Laser Centre, Department of Physics, University of Latvia, Rainis blvd. 19, Riga, Latvia,
LV-1586

*E-mail: inese.birzniece@gmail.com,

Cold/ultracold polar molecules are of great interest due to their promising application in many different fields of physics and chemistry [1]. Prospective polar molecular species for usage in cold/ultracold environment are heteronuclear alkali metal dimers. To realize efficient optical schemes for getting molecules into their rovibronic ground state it is important to have detailed information about the energy levels of excited electronic states with mixed singlet-triplet nature. Among possible candidates to be used as intermediate levels in these optical schemes are low-lying $^1\Pi$ electronic states. We will present the results for the lowest $^1\Pi$ states in KCs and RbCs molecules studied by high resolution spectroscopy Fourier-transform spectroscopy.

In total we have measured and analyzed more than 350 laser induced fluorescence (LIF) spectra from KCs $B(1)^1\Pi$ [2, 3] and $D(2)^1\Pi$ [4] states as well as from RbCs $B(1)^1\Pi$ [5] state. By analyzing the spectra it appeared that, since these excited electronic states are markedly influenced by nearby triplet states, it would be impossible to obtain single-state potential energy curves (PECs) which reproduce the term values with experimental uncertainty (about 0.01 cm^{-1}). As a result, we decided to construct the PECs by using the less perturbed data. In order to select such energy levels for the further fitting procedure, we determined and analyzed the behavior of q -factors and rotational constants B_v .

As a result, we have constructed the PECs for all three investigated electronic states using inverted perturbation approach (IPA) covering $v' = 0 - 35$ with standard deviation (SD) 0.94 cm^{-1} for the B -state in KCs, $v' = 0 - 28$ for the D -state ($\text{SD} = 0.5\text{ cm}^{-1}$) in KCs, and $v' = 0 - 35$ ($\text{SD} = 0.95\text{ cm}^{-1}$) for the B -state in RbCs. The Dunham coefficients set was obtained for the $B(1)^1\Pi$ states of KCs and RbCs molecules. Though the obtained PECs do not reproduce the entire set of energy levels with experimental accuracy, for the lowest vibrational levels ($v' \approx 0-2$) experimental data are described within experimental uncertainty of 0.01 cm^{-1} .

The support from the Latvian Science Council Grant Nr. 119/2012 as well as from Latvian Education and Science Ministry grant Nr. 11-13/IZM14-12 is gratefully acknowledged.

References

- [1] L. D. Carr, D. DeMille, R. V. Krems, and Jun Ye, New Journal of Physics **11**, 055049 (2009)
- [2] I. Birzniece, O. Nikolayeva, M. Tamanis, and R. Ferber, J. Chem. Phys. **136**, 064304 (2012)
- [3] I. Birzniece, O. Nikolayeva, M. Tamanis, and R. Ferber, JQSRT **151**, pages 1-4 (2015)
- [4] I. Birzniece, O. Nikolayeva, M. Tamanis, and R. Ferber, submitted to J. Chem. Phys.
- [5] I. Birzniece, O. Docenko, O. Nikolayeva, M. Tamanis, and R. Ferber, J. Chem. Phys. **138**, 154304 (2013)

Comparison of optimized and most significant illuminants using a spectrally tunable light source

Daiga Cerane^{1,*}, Pauli Fält², Piotr Bartczak²

¹*Department of Optometry and Vision Science, University of Latvia, Kengaraga iela 8, Riga, Latvia, LV-1063*

²*School of Computing, University of Eastern Finland, Joensuu, Finland*

**E-mail: daiga.cerane@lu.lv*

Using a spectrally tunable light source with specified patterns on a DMD (Digital Micromirror Device), light with specific spectral shapes can be created. The light produced is used to illuminate eye through a fundus camera. The image is captured with monochromatic camera. The images of a retina are optimized using MATLAB.

Optimized light spectra for detection of diabetic lesions and retinal landmarks have been created previously [1] - optimized illuminations and their simplified versions (most significant spectral channels).

In the experiment, images are taken using both optimized and most significant lights, then normalized (for exposure time) and compared.

References

[1] Fält P., Hiltunen J., Hauta-Kasari M., Sorri I., Kalesnykiene V., Pietilä J., Uusitalo H., Spectral Imaging of the Human Retina and Computationally Determined Optimal Illuminants for Diabetic Retinopathy Lesion Detection. *Journal of Imaging Science and Technology* **55**, 030509-1 – 030509-10 (2011)

Accommodation lag under monocular and binocular conditions in symptomatic and asymptomatic emmetropes

Karola Panke^{1,*}, Aiga Svede¹, Wolfgang Jaschinski², Gunta Krumina¹

¹*Department of Optometry and Vision Science, University of Latvia, Kengaraga 8, Riga, Latvia, LV-1063*

²*Leibniz Research Centre for Working Environment and Human Factors, Ardeystr. 67, D-44139 Dortmund, Germany*

**E-mail: karola.panke@inbox.lv*

Introduction: Accommodation is the focusing mechanism that provides fast changes in the optical power of the eye in order to keep the image clear when changing the gaze from far to near distance. For each distance there is a constant theoretical accommodative demand, but real accommodation response maintain slightly lower. Difference between accommodative demand and accommodation response is called accommodative lag. The purpose of this study was to estimate the relationship between accommodation lag under monocular and binocular conditions in symptomatic and asymptomatic groups.

Method: Twenty participants (emmetropes) with mean age 24 ± 4 years participated in the study. Accommodative response was measured for dominant eye with open-field infrared autorefractometer (Shin-Nippon, SRW-5000) at 40 cm, 30 cm, and 24 cm (corresponding accommodative demands of 2.5D, 3.33D, and 4.17D) under monocular and binocular condition. Each accommodation measurement consisted of approximately 130 dynamic data points collected during consecutive 2 min time. Dissociated phoria for each distance was measured with Madox test. Convergence insufficiency symptom survey (CISS) score was used to distinguish symptomatic and asymptomatic group. Sequence of accommodation measurements were random order and all experiment was replicated twice within 7 ± 2 days.

Results: The two measurement sessions resulted in a test-retest correlation of $r = 0.95$ for accommodative response. To indicate reliability of accommodation response, we used the standard deviation of the difference between repeated measurements (0.22 D). For asymptomatic group monocular accommodative lag differed significantly across the distances \square from 40 cm to 30 cm (0.22 ± 0.19 D, $p = 0.028$) and from 40 cm to 24 cm (0.35 ± 0.25 D, $p = 0.006$), showing a tendency for accommodative lag to increase with closer distance (nonparametric ANOVA: $p = 0.025$). For symptomatic group monocular accommodative lag differed in similar way - from 40 cm to 30 cm (0.20 ± 0.32 D, $p = 0.02$) and from 40 cm to 24 cm (0.24 ± 0.31 D, $p = 0.02$). Binocular accommodation lag was significantly smaller than monocular accommodation lag (Spearman $r = 0.77$, $p < .001$).

Conclusions: At close working distances (40 cm and closer), accommodation tends to be more variable and inaccurate for symptomatic patients both for monocular and binocular viewing conditions.

Acknowledgements This study is supported by ESF Project No.2013/0021/1DP/1.1.1.2.0/13/APIA/VIAA/001 and also funded by "Deutsche Forschungsgemeinschaft" (DFG JA 747/5-2)

The perception of coherent motion for the centric and eccentric fixation of a stimulus

B.Marcinkevica^{1,*}, E. Kassaliete¹, S. Fomins¹, I. Lacis¹

¹*Department of Optometry and Vision Science, University of Latvia, Riga, Latvia, LV1063*

**E-mail: beata.marcinkevica@gmail.com*

Problem: The ability to perceive the motion of an object is one of the basics of visual perception. The constant change of retinal images depends not only on the movement of objects in various directions and at various speeds, but also on our movement relative to immobile objects. [1] The perception of motion is related to two terms – global motion and local motion. If a point changes its place, it is a local motion. If there are several points, and their vectors become integrated, the perception of a common motion occurs (global motion). [2] Neurones that perceive peripheral retinal information have bigger receptive fields than neurones that receive information from the centre of a retina only. The periphery of a retina allows recognising motion, high perceptibility of contrasts and low spatial frequencies. Central receptive fields recognize colours, low perceptibility of contrast and high spatial frequencies. [3]

Hypothesis: The thresholds of motion perception are lower for the eccentric parts of a retina.

Aim: To analyse, which type of fixation results in the lower thresholds of perception of coherent motion; to evaluate the inaccuracy.

Methods:*Participants:* The experiment involved 7 people. The average age of participants was $19,6 \pm 0,6$ years. *Methodology:* The thresholds of coherent motion were evaluated using RDK (random dot kinematogram). 160 black dots, 7' each (arcminutes), were displayed on a monitor in a $12^\circ \times 12^\circ$ field. The working distance was 60 cm from the surface of the monitor. The motion speed of stimuli was $2^\circ/\text{s}$ with an exposition of 400ms. The evaluation of the threshold was performed using the adaptive staircase psychophysical method. Each participant was measured 5 times for both central and eccentric fixation (12° from the centre). The participant used their dominant eye to perceive the motion.

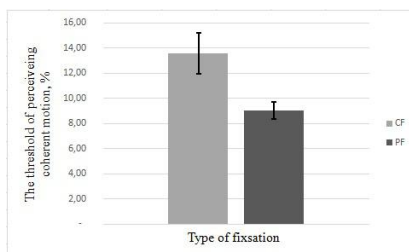


Figure 12: The mean thresholds of the perception of coherent motion for central (CF) and eccentric (PF) fixation.

Results: For two out of seven participants it was proven that the thresholds for central and eccentric fixations are statistically different. In others, a similar pattern was detected, but it could not be statistically proven. The analysis of the mean thresholds for

the perception of coherent motion shows that it is significantly lower ($p < 0,05$) for the eccentric fixation. For central fixation the threshold is $13,6 \pm 1,6\%$, for the eccentric one $-9,1 \pm 0,7\%$. For the first and the fifth analysis using Bland-Altman, there is the effect of learning apparent for central fixation, but not for the eccentric one. The variation of results for 5 measurements is significantly higher for the thresholds for central fixation ($2SD = \pm 14,4\%$) than it is for the peripheral one ($2SD = \pm 4,1\%$) ($p < 0,05$).

Conclusions: The results confirm the hypothesis that states that the peripheral receptive fields perceive the coherent motion better, showing lower thresholds and lower data variation, as well as for the eccentric fixation the effect of learning does not occur. For further research it would be advisable to increase the number of participants and change the methods in order to confirm that the methodology chosen does not affect the results.

Acknowledgement: This study is supported by ESF project No.2013/ 0021/ 1DP/ 1.1.1.2.0/ 13/ APIA/ VIAA/ 001.

References

- [1] Claire V. Hutchinson, Tim Ledgeway, Hrriet A. Allen. The ups and downs of global motion perception. *Frontiers in Aging Neuroscience*, 2014, Vol.6, Article 199, p.1
- [2] Simon J. Crooper. *Motion vision: Local and global motion signals and their interaction in space and time*. Springer Verlag, Berlin Heidelberg New York, 2001. 125 p.
- [3] Jeffrey D. Bower, Zheng Bian, George J. Andersen. Effects of retinal eccentricity and acuity on global motion processing. *Atten Percept Psychophys.*, 2012, Vol.74, p.942-949

Influence of mental fatigue on visual grouping task

Diana Bete^{1,*}, Jurgis Skilters², Vsevolod Liakhovetckii^{1,3}, Gunta Krumina¹

¹University of Latvia, Department of Optometry and Vision Science, Riga, Latvia

²University of Latvia, Center for the Cognitive Sciences and Semantics, Riga, Latvia

³Pavlov Institute of Physiology, Russian Academy of Sciences, St.Petersburg, Russia

*E-mail: diana.bete.inbox.lv

Mental fatigue is a multi-dimensional perceptual and cognitive phenomenon interacting with and having impact on different perceptual and cognitive processes [1]. According to recent research evidence, mental fatigue impacts performance of perceptual and cognitive tasks, decreases the quality and increases the amount of errors [2]. In our study we investigate the impact of mental fatigue on the execution of visual grouping task in general and attentional processes that are implemented while doing it in particular. Visual grouping is usually executed according to different features, for example, colour or shape. The aim of our study is to assess the time for making visual attention task and to explore the correlation between the amount of mistakes and the level of subject's tiredness. Further, we also attempt to assess how a particular part of day (when the test is conducted) influences the performance of grouping task.

Research was conducted by using onscreen grouping task. Subjects did 4 grouping tasks, where the instruction was to find objects with aperture in the same direction. Every task consisted of 10x8 objects. 60 test subjects, between 18 and 32 years old, took part in research. Subjects also answered some general questions about their health and general feeling.

Results show, that grouping tasks can be completed faster, if there are more than one grouping feature – objects are in the same direction and in the same colours which might be interpreted as a result of additional configurational effects. But grouping task is performed slower if objects in the same direction are in different colours (which might be interpreted as a result of two different competing processes of grouping, i.e., similarity in shape and similarity in colour). Time for task execution more increases for those subjects who feel tired than those who indicated that they feel lively and are not tired. Tired subjects also made more mistakes. According to our results, the results of the test executed in the evening are the shortest if compared with other daytimes.

Mental fatigue has an impact on visual grouping task. Mentally fatigued subjects need more time to complete the test, and they also do more errors than those who are not tired. The results of our research also shows that the task is faster if conducted in the evening. Impact of the time if the test is conducted in the morning, at day and at night are not statistical significant for the test performance. Finally, according to our results, we can argue that grouping is better if there are more than one feature for grouping (i.e., configurational effects enhance the processes of grouping and attention).

The study was supported by ESF No.2013/0021/1DP/1.1.1.2.0/13/APIA/ VIAA/001.

References

- [1] DeLuca, J. (Ed.) , *Fatigue as a window to the brain*. (Cambridge, MA: MIT Press, 2007)
- [2] Faber, L.G., Maurits, N.M., Lorist, M.M. Mental fatigue affects visual selective attention, *PloS one* **7**(10), e48073 (2012)

Dust particle laser detection in laboratory air

Janis Alnis¹, Jazeps Rutkis¹,

¹ *Institute of Atomic Physics and spectroscopy University of Latvia, Riga Latvia E-mail: jazepsrutkis93@gmail.com*

Dust particles in the air are one of major obstacles in high power laser spectroscopy involving optical resonators. Usually in laser laboratory air conditioning using filtration is necessary. This is especially important if laboratory is situated in urban environments where besides dust carbon soot nanoparticles are present from car exhaust and furnaces.

Air cleanness is also important in medical aspect - pollen from grass, flowers and trees in nature is causing asthma and allergies for some people [1].

We examined the air quality using a commercial dust sensor (Sharp GP2Y10) using an Arduino board for data recording and analysis. A fan was used to accelerate the air flow through the sensor. The data was displayed using an LCD monitor. We found the precision was not sufficient for our application, so we constructed a custom sensor.

In our custom-built sensor a 1W laser diode light was directed at the particles and Mie scattering was observed and recorded by a digital camera. The camera's data was processed using LabVIEW image processing tools. This allowed us to achieve a high precision in detecting both the size and number of the dust particles.

Using this sensor we were able to evaluate the cleanliness of the air as well as the efficiency of several air filtering methods.

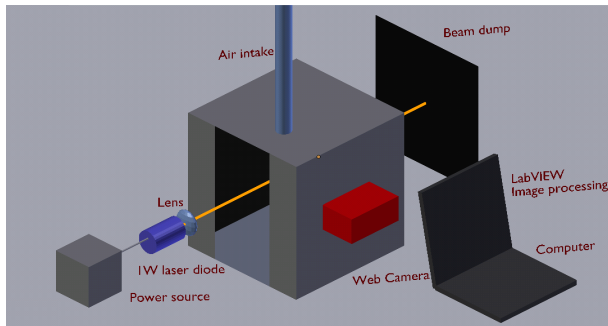


Figure 13: Custom built particle sensor

References

[1] J. Sandsten et al, Single aerosol particle sizing and identification using a coupled cavity diode laser, Opt. Comm. 168 17-24 (1999).

Smart model eye on base of polymer dispersed liquid crystals and CMOS sensor

Maris Ozolinsh^{1,2}, Paulis Paulins,² and Varis Karitans¹

¹*Institute of Solid State Physics, University of Latvia, Kengaraga 8, Riga, Latvia, LV-1063*

²*Department of Physics and Mathematics, University of Latvia, Zellu 8, Riga, Latvia, LV-1002*

**E-mail: ozoma@latnet.lv,*

We report on developed model eye for studies of deterioration of image quality, optical system resolution, modulation transfer function in cataract eye lens using a polymer dispersed liquid crystal (PDLC) cell [1] as smart media. The model allows the electrical field inducing of scattering that corresponds to various levels of cataract. Since now different media are used for alternating of scattering efficiency (i.e., no smart media, but model with alternate scattering – (Donnelly, 2005) in model eyes [2]). Previously we have demonstrated the controlling of “cataract” scattering efficiency in visible by applying the AC electric field to a thin PDLC layer [3]. The model eye is built using CMOS sensor built in PANASONIC Lumix LX1 camera with a sandwich element comprised of two glass plates with a light scattering PDLC layer filled between. The compound is built in a special adapter. The lens module (on the base of Sigma 24mm Olympus OM Filtermatic with effective f-number $F = 2.8$) is mounted on the platform of digital photcamera - horizontal sensor pixel pitch $1.4 \mu\text{m}$, digital output 14-bit depth. Camera has full manual operation and allows to select exposure 1/4000 to 60 s. Applying the AC electric field up to 30V continuously diminishes scattering efficiency. Model eye properties were tested regarding to image point spread function PSF and image line spread function LSP, eye “contrast vision function” in presence of simulated in PDLC light scattering. Light scattering effect on detectability of model eye lens aberrations using Shack-Hartman sensor is in progress.

References

- [1] H. Ramanitra, P. Chanclou, L. Dupont, and B. Vinouze, *Optical Engineering* **43**(6), 1445-1453 (2004)
- [2] W. J. Donnelly (2005); voi.opt.uh.edu/VOI/WavefrontCongress/2005/presentations/19-Donnelly-Scatter.pdf
- [3] J.M. Bueno, M. Ozolinsh, and G. Ikaunieks, *Ferroelectrics* **370**, 18-28 (2008)

"Variantor" functional spectral filter that stimulates trichromats see as dichromats

Zane Jansone¹ and Maris Ozolinsh^{1,2}

¹*Dept of Optometry and Vision science, University of Latvia, Kengaraga 8, Riga, Latvia, LV-1063*

²*Inst. of Solid State Physics, University of Latvia, Kengaraga 8, Riga, Latvia, LV-1063*

**E-mail: ozoma@latnet.lv,*

"Variantor" functional spectral filter helps people with normal color vision to understand what the world looks like to color deficient people and which color combinations are confusing for these people [1]. In our study we tested the characteristics of these glasses: their spectrum of absorption; effectiveness of the color transfer and the patient response looking through the goggles on different color images. Their use was tested using color tests - Ishihara pseudoisochromatic plates and anomaloscope. The main goal was to test the "Variantor" effectiveness in everyday life.

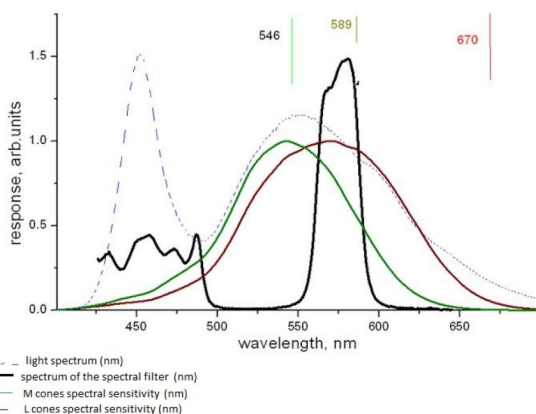


Figure 14: Spectral characteristics of filters and eye cone sensitivities

"Variantor" absorbed spectrum from 495nm till 555nm. In our research participated 3 observers: 1 trichromat, a person with deuteranomaly and a trichromatic person wearing glasses. During the studies (color discrimination of Ishihara plates) the results showed that person with "Variantor" response was much slower and it was more difficult to distinguish different color objects. Results showed that anomaloscope can't be applied to the test - are the patients trichromats or dichromats, because color stimuli used in anomaloscopes are monochromatic (see marks in the upper part of Fig.1); and they belong to the spectrum range which is absorbed the filter. Author M.O. was supported by ESF project No.2013/0021/1DP/1.1.1.2.0/13/APIA/VIAA/001.

References

[1] S. Nakauchi, T. Onouchi, H. Katou, H. Oda, Y. Saitou, and K. Miyazawa. US Patent App.12/223,317; July 15 2010

High Speed Single Photon Detector

Astghik Kuzanyan*, Armen Kuzanyan

Institute for Physical Research NAS of Armenia, Ashtarak-2, Ashtarak, Armenia, 0203

**E-mail: astghik.kuzanyan@gmail.com,*

Cryogenic thermoelectric single-photon detectors (TSPD) are one of the emerging techniques for fast single-photon counting. Single-photon detectors are required for research in different areas of modern science, particularly in space astronomy, high energy physics, quantum computing and quantum cryptography. The principle of operation of the TSPD is simple. Sensor of a TSPD consists of two absorbers and a connecting thermoelectric bridge. When one of the absorbers absorbs a photon, its temperature increases by an amount proportional to the energy of the absorbed photon. The resulting temperature difference between the ends of the thermoelectric bridge creates a potential difference. We can measure potential difference with great precision and thus register an absorbed photon and determine its energy. We have collected and analyzed the values of thermoelectric parameters of thermoelectric materials and on this basis calculated the photon count rate of the Thermoelectric Nanowire Single-Photon Detector (TNSPD). It is concluded that the TNSPD can achieve higher specifications as compared with the best single-photon detectors. The lanthanum-cerium hexaboride sensors of TNSPD are expected to reach more than gigahertz count rates.

References

- [1] A.Gulian, K.Wood, D. Van, G. Fritzed, Journal of Modern Optics, **51**, 1467-1490 (2004)
- [2] A.A. Kuzanyan, V.A. Petrosyan, A.S. Kuzanyan, Journal of Physics: Conference Series, **350 012028**, (2012)

EPR investigation of Gd^{3+} local structure in ScF_3

Andris Antuzevics*, Uldis Rogulis, Juris Purans

Institute of Solid State Physics, Kengaraga 8, Riga, Latvia, LV-1063

**E-mail: andris.antuzevics@gmail.com,*

ScF_3 is a fluoroperovskite with simple cubic structure that has a negative thermal expansion (NTE) coefficient. Studies of Gd^{3+} centres in similar materials with positive thermal expansion coefficient have revealed a temperature dependence of zero field splitting (ZFS) parameters. [1]

In this work ZFS of Gd^{3+} impurity in ScF_3 is studied by electron paramagnetic resonance (EPR) at 77 and 295 K. Spin-Hamiltonian parameters are determined with high precision from the EPR spectra angular dependence simulations.

Regardless of NTE the temperature dependence of ZFS parameters in ScF_3 is similar to other cubic fluoroperovskites. Separation of thermal expansion and spin-phonon contributions to ZFS values reveal that although the bulk crystal has a NTE coefficient, the local structure of Gd^{3+} centres expands positively with temperature. The result is consistent with EXAFS studies of average instantaneous distance R between atoms in crystals with NTE coefficient. [2] Perpendicular vibrations of atoms effectively increase R causing positive thermal expansion of the local structure. We can conclude that EPR parameters correlate with R values, not crystallographic distances between atoms measured by diffraction.

References

- [1] T. Rewaj, M. Krupski, J. Kuriata, J. Y. Buzare, J. Phys. Condens. Matter **4**, 9909-9918 (1992)
- [2] P. Fornasini, N. Abd el All, S. I. Ahmed, A. Sanson, M. Vaccari, Journal of Physics: Conference Series **190** (2009)

Adaptive optics for better vision

Pabo Artal

Laboratory of Optics, Murcia University, Spain

E-mail: pablo@um.es,

Different laboratories in the world developed adaptive optics (AO) instruments for use in Ophthalmology. The main application in the early days of AO for the eye was to improve the resolution and quality of retinal images recorded through the corrected eye's optics in ophthalmoscopes. However, once AO instruments were operative for the eye, we soon realized that not only ocular aberrations could be corrected, but also any desired aberration pattern could be added to the eye in a controlled manner. By using an additional optical path, visual stimuli were projected to the eye's subject to perform visual testing for a variety of optical conditions. This is the basis of the concept of the adaptive optics vision analyzer. This instrument consists of a wavefront sensor to measure the eye's aberrations and a correcting device to modify the eyes optics. The correcting/manipulating device is placed in the system conjugated both with the subject's pupil plane and the wavefront sensor, by using appropriate sets of lenses in a telescope configuration. Subjects view a stimulus (letters or any visual scene) produced by a micro-display. The potential applications of this type of AO instruments in Ophthalmology can be enormous. Perhaps the most obvious is the progressive substitutions of phoropters, those old-fashion systems that you find in any ophthalmic clinic, containing wheels with different lenses used during visual testing to determine the required optical prescription. With AO, standard lenses will be replaced with opto-electronics devices and moreover, not only defocus and astigmatism, but all optical aberrations could be induced. This will allow optimizing the optical correction for different visual tasks. For example, in some cases, some residual customized amount of spherical aberration could provide some extra depth of focus in presbyopic eyes. Another powerful application will be the pre-testing of different optical solutions. In invasive procedures, such as laser refractive surgery, before a definitive ablation of the cornea is performed, the optical profile to be induced could be optimized for each patient. This will open the door to an era of true customized eye treatments. The future of this technology looks promising and I expect a rapid transition from the laboratories to the clinics. However, there are challenges that still need substantial work. Although we have already proposed binocular AO systems, they are still limited to the laboratory. An additional advance for this field will be the reduction of the associated costs of the key correcting elements. The high costs of these technologies today lay at the limit of what is commercially viable for clinical instruments. I am convinced that these tools will revolutionize the way vision is tested and corrected today. A revision of the history of the field and the current state of the art will be presented.

Measurement of the thickness of the corneal tear-film using a Twyman-Green interferometer

Varis Karitans¹, Inta Silina², Juris Lukjanovs², Gunta Krumina²

¹Department of Ferroelectrics, Institute of Solid State Physics, University of Latvia,
Kengaraga street 8, Riga, Latvia LV-1063

²Department of Optometry and Vision Science, Faculty of Physics and Mathematics,
University of Latvia, Kengaraga street 8, Riga, Latvia, LV-1063

*E-mail: variskaritans@gmail.com,

Non-invasive optical methods such as the optical interferometry and reflectometry become increasingly popular for studies of the corneal tear-film [1, 2]. In this study, we develop a Twyman-Green interferometer that could be used to measure the thickness of the tear-film. The optical system shown in Fig. 21 makes use of interference of rays reflected from the surface of the tear-film and the tear-film and cornea interface.

However, apart from the study [1] the rays hit the surface of the tear-film at normal angle reducing influence of head and eye movements on the results. Fig. 15b shows the tear-film interference measurements of one subject. Periodical variations in the relative intensity can be noticed suggesting that the method used can be applied for measuring the tear-film thickness.

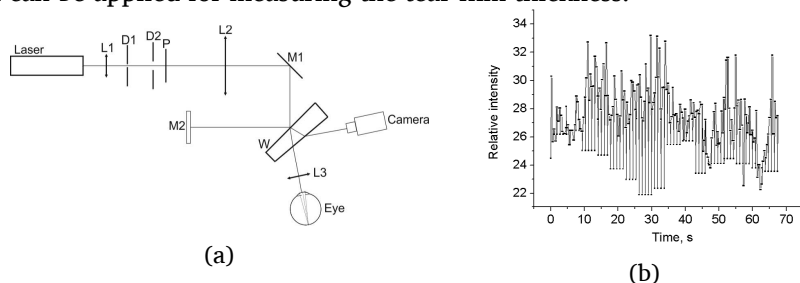


Figure 15: (a)The optical system used in the study. L denotes lens, M denotes mirror, D denotes diaphragm, P denotes polarizer, W denotes wedge. (b) Variations in relative light intensity in time.

In Fig. 15b only a portion of all the trace of variations is shown. The data appears noisy and this is most likely due to low signal-to-noise ratio (SNR), various kind of noise etc.

References

- [1] J. I. Prydal, F. W. Campbell, Investigative Ophthalmology and Visual Science **33**, 1996-2005 (1992)
- [2] H. Lu, M. R. Wang, J. Wang, M. Shen, Journal of Biomedical Optics **19**, 027001-1-027001-8 (2014)

Axial eye elongation and changes in refraction error for myopic European children using custom-made overnight orthokeratology contact lenses

Janis Baltraitis^{1,*}, Viktorija Vlasenko¹, Laura Vilkausa¹, Raimonds Rogulis¹, Dace Erenbote¹, Andrej Solomatin², Ivars Lacis³,

¹*Gallus Optika, Antonijas 24, Riga, Latvia, LV-1010*

²*Dr.Solomatina acu rehabilitācijas un redzes korekcijas centrs, Elizabetes 75, Riga, Latvia, LV-1050*

³*Department of Optometry and vision science, University of Latvia, Rainis blvd. 19, Riga, Latvia, LV-1586*

*E-mail: janis.baltraitis@gallus.lv,

Purpose The prevalence of myopia in young adolescents has increased substantially in recent decades and has approached 10 to 25 and 60 to 80 (percent) in industrialized societies of the West and East Asia, respectively. Furthermore, high levels of myopia are associated with a range of ocular pathologies, such as vitreous and retinal detachment, macular degeneration, and glaucoma. Therefore, myopia can incur significant ocular-related morbidity and substantial health-care costs. [1].

Research Most of the researches are done in Asia, so each Europe based research is vital to obtain more proofs and give a place for discussions. Examinations of myopic under 12 years old overnight orthokeratology contact lens wearers have shown stabilization on changes of refractive error. To get deeper understanding and obtain objective evidences, 11 subjects (22 eyes) are randomly assigned for this research since July 2014.

Method Axial length measurements are done each 6 month after proper fit contact lens has been approved to give a full correction. Axial length is measured with non-contact method using Zeiss IOL-Master. Besides this, is measured thickness and changes of sclera using Zeiss OCT technology. Cycloplegical overrefraction is done annually. Eye health, contact lens fit, overrefraction examinations are scheduled in the morning and afternoon check-ups according to contact lens fit plan.

Results Correlation amount by factors like: - refraction error and axial length; - refraction and thickness of sclera; - myopia development and change of axial length; - myopia development and thickness of sclera; - myopia development and changes in thickness of sclera. First comparable results of anatomical changes will be ready after examinations in February 2015. Meanwhile, we can analyse refractive changes prior orthokeratology fit and compare to the results with orthokeratology. Results will be comparable to the research - Myopia Control with Orthokeratology Contact Lenses in Spain: Refractive and Biometric Changes [1].

References

[1] J. Santodomingo-Rubido, C. Villa-Collar, B. Gilmartin, R. Gutierrez-Ortega, Investigative Ophthalmology and Visual Science **Volume 53, No.8**, 5060-5065 (2012)

System for melanopsin related pupillometry

Sergejs Fomins¹, Brigita Zutere², Gunta Krumina^{2,*}

¹*Institute of Solid State Physics, Kengaraga 8, Riga, Latvia, LV-1063*

²*Biology Faculty, University of Latvia, Kronvalda bld. 4, Riga, LV-1010*

³*Optometry and Vision Science Dept., University of Latvia, Kengaraga 8, Riga, Latvia, LV-1063*

*E-mail: sergejs.fomins@gmail.com

The retina of primates contains intrinsically photosensitive retinal ganglion cells. Pigment melanopsin originated in this cells is most sensitive to blue light and helps to controls the pupil reactions together with cones signal.[1] To investigate the contribution of melanopsin to daytime cycle and pupil response, we have developed the infrared pupil monitoring system. The system comprises wide field integrating sphere for efficient stimulation of the retina. The pupil is illuminated with 850 nm near infrared power led. Pupil is monitored with the high frame rate IR camera. Pupil tracking and diameter calculations are applied through C++ Open CV routines.

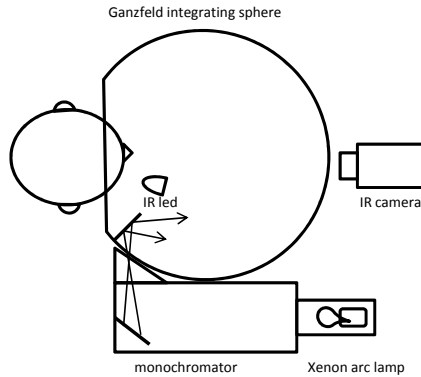


Figure 16: Diagram of the experimental electro-optical setup for eye pupil measurements. Eye pupil monitoring via infrared light. Visible stimuli is provided via monochromator.

Xenon arc lamp is used as a light source for monochromator. To introduce the modulation of light, mechanical switch is placed between the monochromator and integration sphere. The switch is a disk with holes shaped to produce the sinusoidal changes of the light intensity in the sphere.

Acknowledgement

This study is supported by ESF project No.2013/0021/1DP/1.1.1.2.0/13/APIA/VIAA/001.

References

[1] Barrionuevo PA, Nicandro N, McAnany JJ, Zele AJ, Gamlin P, Cao D., Invest Ophthalmol Vis Sci. 55, 719-727 (2014)

Perception of biological motion in central and peripheral visual field

Ilze Laicane^{1,*}, Jurgis Skilters², Vsevolod Lyakhovetskii^{1,3}, Elina Zimasa¹, Gunta Krumina¹

¹*Department of Optometry and Vision Science, University of Latvia, Kengaraga 8, Riga, Latvia, LV-1063*

²*Department of Communication Science/ Center for Cognitive Sciences and Semantics, University of Latvia, Lomonosova 1A, Riga, Latvia, LV-1019*

³*Pavlov Institute of Physiology, Russian Academy of Sciences, St.Petersburg, Russia*

*E-mail: ilze.laicane@lu.lv,

One of the most intriguing categories in motion analysis is the movement of a living organism. Swedish psychophysicist Gunnar Johansson (1973) was the first who noted that in order to perceive motion of the whole human body it was sufficient to demonstrate only the movement of its major joints [1]. Although biological motion has been widely studied, it is not entirely clear (a) whether the perception of biological motion is equally precise across all visual field [2,3] and (b) what is the underlying mechanism that determines central and eccentric motion perception of a biological object. The aim of this research work was to analyze the eccentric perception of visual motion when limited information of the movement is given.

In a psychophysical experiment the participants were instructed to determine whether the presented stimulus is a biological object walking in any of five different directions or a scrambled version of the object. The number of dots representing the motion varied from 1 to 13 according to staircase method. The stimulus demonstration sequence was generated based on adaptive staircase block up-down temporal interval forced-choice method BUDTIF [4].

Preliminary results indicate that perception of biological motion in the central visual field is highly individual (average thresholds range from 3.8-7.1 points, SEs range from 0.1-0.4 points). Perceptual learning is not observed during the performance of 10 sequential tests. The results demonstrate that the chosen experimental setting is applicable for the evaluation of perceptual processes of biological motion.

Study is supported by ESF project No.2013/0021/1DP/1.1.1.2.0/13/APIA/VIAA/001

References

- [1] Johansson, G., Visual perception of biological motion and a model for its analysis. *Perception and Psychophysics*, **14**, 201-211, (1973)
- [2] Gurnsey, R., Roddy, G., Troje, N. F., Limits of peripheral direction discrimination of point-light walkers. *Journal of Vision*, **10(2):15**, 1-17, (2010)
- [3] Ikeda H., Blake R., Watanabe K., Eccentric perception of biological motion is unscalarmy poor. *Vision Research*, **45**, 1935–1943, (2005)
- [4] Campbell, R., A., Lasky, E., Z., Adaptive Threshold Procedures: BUDTIF. *The Journal of the Acoustical Society of America*, **44(2)**, 537-541, (1968)

Visian ICL: intraocular collamer lens for refractive correction

Evija Gulbinska
Latvian American Eye Center
E-mail: evija@laac.lv,

ICL is an intraocular lens which is made from a special biocompatible material - collamer that is known as human body-friendly material.

Collamer contains some collagen which repels protein molecules and attaches a monolayer of fibronectin, as a result the eye does not perceive ICL as a foreign body, thus minimizing the inflammation risk. Collamer is characterised by good flexibility, therefore ICL lens is used as a folded lens which is introduced into the eye through a small (3mm) incision between the iris and the crystalline lens of the eye near the external border of the cornea where it fully opens easily and predictably and can stay permanently without any care.

Visian ICL offer includes full range of correction from -18 to + 10 D with or without astigmatism up to 6 D and this method is reversible- the lens can be removed or changed if it is necessary.

Visian Toric ICL has proven to provide excellent predictability, efficacy and safety with good reduction of preoperative refraction and stability over time

Visian ICL is also a good alternative for patients who are not candidates to LASIK because of dry eye or thin cornea.

Estimation of the effect of Cs and Sr salts on Brassica napus

L. CFI parameters using "Floratest" optical biosensor

I. Burkova^{1,*}, K. Shavanova², O. Pareniuk^{2,*}, V. Illienko¹, M. Taran¹, N. Starodub¹

¹*National University of Life and Environmental Sciences of Ukraine, Heroyiv Oborony st., 15, Kyiv-03041, Ukraine.*

²*Institute of Environmental Radioactivity of Fukushima University, 1 Kanayagawa, Fukushima City, Fukushima Prefecture, 960-1296 Japan*

**E-mail: inna.burkova@ukr.net,*

The results of rape (*Brassica napus* L.) sensitivity to stress factors like metal salts, using "Floratest" fluorometer are considered in the following article. The method of chlorophyll induction of fluorescence is showing the integral photosynthesis intensity and the state of plants' photosynthetic membranes. The aim of research was to determine the parameters of chlorophyll fluorescence induction curve for rape plants (*Brassica napus* L.), which were grown in the presence of metals salts - CsCl, SrCl₂, KCl, CaCl₂ (concentrations – 0,2 mM, 2 mM and 0,02 M). Rape (*Brassica napus* L.) was chosen to be the object of the research. Rape seeds were preliminary soaked in a metal salts solution. In the process of rape vegetation, we tracked changes of chlorophyll fluorescence induction performances. As a result of research, it was determined that the most stressful factors for rape plants are CaCl₂ (0,02 M) and CsCl (0,02 M) salts, because the number of inactive chlorophyll increased. All studied concentrations of SrCl₂ partially suppressed the fluorescence.

Investigation of skin autofluorescence lifetime under optical irradiation

Antra Dzerve¹, Inesa Ferulova¹, Alexey Lihachev¹ and Janis Spigulis¹

¹*Institute of Atomic Physics and Spectroscopy, University of Latvia, Rainis blvd. 19, Riga, Latvia, LV-1586*

**E-mail: antra_dzerve@inbox.lv,*

The autofluorescence lifetime of healthy human skin was measured using excitation provided by picosecond diode laser and fluorescence emission was collected in visible range. In addition, spectral and temporal responses of healthy human skin in vivo were studied before and after photobleaching. Photobleaching is the decrease in the intensity of skin autofluorescence during temporally stable irradiation[1]. A change in the autofluorescence lifetimes was observed after photobleaching of human skin. A three-exponential model was used to fit the signals, the data were processed by TRES (Time-resolved Emission Spectra) and TRANES (Time-Resolved Area-Normalised Emission Spectra)[2] which allows to conclude that there are structural changes in fluorophores due to continual optical irradiation.

References

[1] A. A. Strattonnikov, V. S. Polikarpov, V. B. Loschenov, "Photobleaching of endogenous fluorochroms in tissues in vivo during laser irradiation", *Proc. SPIE*, **Vol. 4241**, 13–24 (2001)

[2] A.S.R.Koti, M.M.Krishna, "*Time-Resolved Area-Normalized Emission Spectroscopy (TRANES): A Novel Method for Confirming Emission from Two Excited States*" (*J. Phys. Chem. A*, 105, 1767-1771 (2001).)

Optical and photoelectrical properties of DMABI chromophore consisting molecules

Julija Pervenecka*, Raitis Grzibovskis, Aivars Vembris

Institute of Solid State Physics, Kengaraga 8, Riga, Latvia, LV-1063

**E-mail: j.kimmi@inbox.lv*

Energy levels provide information about material compatibility with other materials. Therefore determination of energy levels structure of molecules is very important to create high-efficiency device.

In this work optical and photoelectrical properties of dimetilaminobenzylidene-1,3-indandione (DMABI) and four its derivatives were studied. Thin films were made by two methods: spin-coating and thermal evaporation in vacuum. Preparation method was chosen depending on compounds ability to form thin amorphous films from solution.

Thin films with the thickness of 100 nm on quartz glass were prepared for absorption measurements which provide information about optical gap of organic compound.

Studied compound thin films were coated on ITO covered glass for photoemission quantum yield measurements. Additional semi-transparent aluminium electrode was deposited on organic layer for photoconductivity measurements. The thickness of organic layer was measured by Veeco Dektak 150 Surface profilometer and was between 500 and 700 nm.

Both photoemission quantum yield and photoconductivity measurements were performed with the same equipment in vacuum (1×10^{-5} mbar) cryostat. As a light source was used ENERGETIQ Laser Driven Light Source (LDLS EQ-99) with spectral range from 170 nm to 2100nm. Wavelength was changed by MYM-1 diffraction grating monochromator with spectral width of 2nm. Keithley 617 electrometer was used as voltage source and electric current measurements.

The molecule ionization energy in thin films of the studied compounds was obtained by photoemission quantum yield spectroscopy method.

The photoconductivity threshold value was determined from the photoconductivity spectral dependence.

An electron affinity level value was calculated from molecules ionization energy and photoconductivity threshold value.

Information about morphology of the all prepared samples were obtain by optical microscope. Polycrystalline structure was observed from thermally evaporated films and amorphous structure from spin-coated films.

Relation between the studied molecules structure, their optical properties and energy levels will be discussed in the presentation.

Properties of zinc oxide thin films synthesized by extraction-pyrolytic method

Olga Kiselova^{1*}, Antons Cvetkovs², Uldis Rogulis¹, Vera Serga², Reinis Ignatans¹, Karlis Kundzins¹

¹*Institute of Solid State Physics, Kengaraga 8, Riga, Latvia, LV-1063*

²*Institute of Inorganic Chemistry, Riga Technical University, Salaspils, Miera 34, Latvia, LV-2169*

*E-mail: olga.kiselova@gmail.com,

Zinc oxide (ZnO) is very promising material for semiconductor devices. Because of ZnO crystal structure parameters, wide direct band gap (3.37 eV at room temperature) and large exciton binding energy (60 meV) material has good optical, electrical, piezoelectrical and magnetic properties. These properties make ZnO as an important material with a variety of applications, such as a photodetector, light-emitting diodes, gas sensors, biosensors, solar cells, etc. Properties of material can be changed by doping different chemical elements impurities [1].

In the present study thin films of pure ZnO and doped with 10% cadmium oxide (CdO) were synthesized by extraction - pyrolytic method [2] on glass and quartz substrates. The x-ray diffraction (XRD), the thickness and the surface morphology of thin films were measured. XRD patterns showed crystalline phases of ZnO and CdO in the thin films. Size of crystallites are 20 – 60 nm. Morphology of surfaces showed that coating of thin films is non-homogenous.

References

- [1] U. Ozgur, Ya I. Alivov, A. Teke, M. A. Reshchikov, S. Dogan, V. Avrutin, S.-J. Cho, H. Morkoc, J. Appl. Phys. **98**, 041301 (2005)
- [2] A. I. Kholkin, T. N. Petrusheva, *Extractive-pyrolytic method: Production of functional oxide materials* (Moscow: ComBook, 2006)

Alignment-to-orientation conversion due to hyperfine Paschen-Back type angular momentum decoupling in atomic rubidium

M. Auzinsh, A. Berzins, R. Ferber, F. Gahbauer, L. Kalvans, A. Mozers*, A. Spiss

Laser Centre, University of Latvia, Rainis blvd. 19, Riga, Latvia, LV-1586

*E-mail: art.mozers@gmail.com,

We studied alignment-to-orientation conversion [1,2] caused by excited-state level crossings in a nonzero magnetic field of both atomic rubidium isotopes. Experimental measurements were performed on the transitions of the D_2 line of rubidium. These measured signals were described by a theoretical model [3] that takes into account all neighboring hyperfine transitions, the mixing of magnetic sublevels in an external magnetic field, the coherence properties of the exciting laser radiation, and the Doppler effect. In the experiments LIF components were observed at linearly polarized excitation and their difference was taken afterwards. By observing the two oppositely circularly polarized components we were able to see structures not visible in the difference graphs, which yields deeper insight into the processes responsible for these signals (see Fig. 21). We studied how these signals are dependent on laser power density and how they are affected when the exciting laser is tuned to different hyperfine transitions. The comparison between experiment and theory was carried out fulfilling the nonlinear absorption conditions.

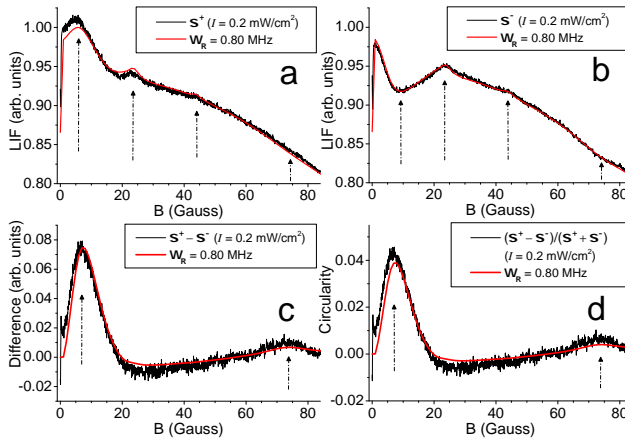


Figure 17: Relative intensities of the two oppositely circularly polarized fluorescence components (a) and (b), their difference (c), and the circularity value (d) for the $F_g = 2 \rightarrow F_e = 2$ transition of ^{85}Rb .

References

- [1] Alnis, Janis and Auzinsh, Marcis, Phys. Rev. A **63**, 023407 (2001)
- [2] Auzinsh, Marcis and Budker, Dmitry and Rochester, Simon M, *Optically polarized atoms: understanding light-atom interactions* (Oxford University Press, Oxford 2010)
- [3] Blushs, Kaspars and Auzinsh, Marcis, Phys. Rev. A **69**, 063806 (2004)

Spectroscopic studies of cadmium containing high frequency electrodeless light sources

Madara Zinge¹, Emils Gosko^{*1}

¹*Institute of Atomic Physics and Spectroscopy, University of Latvia, Skunu str. 4, Riga, Latvia, LV-1050*

**E-mail: emils.gosko@gmail.com*

High frequency electrodeless lamps (HFEDL) are widely used as bright radiators of narrow and intense spectral lines in different types of scientific devices, for instance, in atomic absorption spectrometers. These light sources are manufactured at the Institute of Atomic Physics and Spectroscopy, University of Latvia. HFEDL is a spherical lamp vessel with diameter of 1 cm made of SiO₂ glass and filled with desired working elements and buffer gas.

In this work, plasma under study are four HFEDLs with different fillings: (1) Cd + Ar, (2) Cd + Zn + SbI₃ + Ar, (3) Cd + SbI₃ + Ar and (4) Cd + Zn + Ar (approximate buffer gas pressure 3 Torr).

An inductively coupled discharge is induced by placing lamp in electromagnetic field of frequency 250 MHz. The emission spectra of the discharge were registered by means of Jobin Yvon SPEX 1000M high resolution spectrometer (grating 1200 l·mm⁻¹) and charge coupled device matrix detector (Symphony, 2048×512 Thermoelectric Front Illuminated UV Sensitive CCD Detector). AVANTES AVS-PC2000 plug-in spectrometer with 2048 element linear CCD array detector was used to register full spectra (spectral range 200-850 nm) and for intensity stability measurements.

HFEDLs were operated at different excitation generator voltage values (22-29 V), and the emission spectra changes were analyzed depending on gas mixture. Results show that by increasing the generator voltage, the cadmium atomic line intensity increases, but the argon atomic line intensity decreases. In emission spectra of Cd + SbI₃ + Ar HFEDL molecular spectra of OH can be observed which can be used for rotational temperature determination.

Optical vortex trajectory inside the beam focused by an axicon

Mateusz Szatkowski^{1,*}, Jan Masajada¹, Agnieszka Popiolek-Masajada¹

¹*Chair of Optics and Photonics, Wrocław University of Technology, Wyb. Wyspiańskiego 27, Wrocław, Poland*

**E-mail: mat.szatkowski@gmail.com,*

The question of the optical vortex trajectory plays important role in optical vortex scanning microscope [1]. Optical vortex is a stable phase dislocation. In our experiment optical vortex is generated by spiral phase plate (vortex lens), which is mounted on the motorized stage. By shifting vortex lens one can easily move the vortex inside the beam [2]. The line along the vortex move, inside the beam, is called a vortex trajectory. The range of the vortex shift measured at the sample plane is reduced few hundred times, comparing to the vortex lens shift [3]. When there is no object at the sample plane, the vortex point moves along the straight line. The inclination of this trajectory depends on the observation plane position. Optical vortex has the highest sensitivity, when its trajectory is perpendicular to the vortex lens shift, we call this position of the observation plane: a critical plane. Critical plane is situated close to the focus of the microscopic objective. In the present experiment the objective was substituted an axicon (Fig. 21) and an inclination of the optical vortex trajectory for different observation plane positions were measured. Axicon as an optical element with simple geometry [4, 5] could open possibility for better understanding optical vortex trajectory behavior. The results of this experiment and optical vortex trajectory analysis method will be presented.

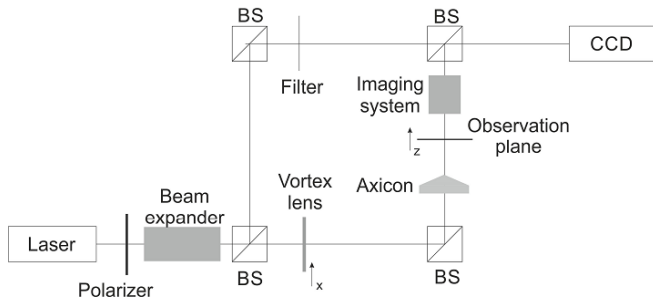


Figure 18: Experiment setup.

References

- [1] I. Augustyniak, A. Popiolek-Masajada, J. Masajada, S. Drobczyński, *Applied Optics* **51**, C117-C124 (2012)
- [2] J. Masajada, M. Leniec, I. Augustyniak, *Journal of Optics* **13** (2011)
- [3] J. Masajada, I. Augustyniak and A. Popiolek-Masajada, *Journal of Optics* **15** (2013)
- [4] Z. Jaroszewicz, A. Burvall, A. T. Friberg, *Optics and Photonics News* **16**, 34-39 (2005)
- [5] Z. Jaroszewicz, A. Burvall, A. T. Friberg, *Applied Optics* **16**, 4838-4844 (2004)

Impact of fatigue on spatial language and cognition

Evija Ziba¹, Jurgis Skilters², Vsevolod Liakhovetckii^{1,3}, Gunta Krumina¹

¹University of Latvia, Department of Optometry and Optical Science

²University of Latvia, Center for the Cognitive Sciences and Semantics, Riga, Latvia

³Pavlov Institute of Physiology, Russian Academy of Sciences, St.Petersburg, Russia

*E-mail: ziba.evija@gmail.com,

Language is used to describe relations between objects in space. When describing these relations, speaker should chose the most appropriate linguistic representation to avoid increased comprehension time and ambiguities. In the present study we examined relationship between fatigue and spatial language. Although fatigue impacts various perceptual and cognitive processes, there are no studies exploring the relationship between fatigue and spatial language. There are also no studies on the representation of spatial relations in Latvian. The goal of our study was to evaluate the effect of fatigue on the spatial language. The main tasks was (1) to compare language-specific properties in Latvian and English spatial prepositions, (2) to discover possible differences between the results when conducting experiment at different times of the day, (3) to find possible differences in spatial perception in the conditions of fatigue.

56 subjects took part in experiment; 22 of them indicated that they feel tired in the beginning of tests, 18 were not tired and 16 participants were neutral in terms of fatigue. The test was conducted in four different times of the day. We used the acceptability rating task (modified from *Logan and Sadler*, 1996) with Latvian spatial prepositions. Picture with configuration of spatial objects and a corresponding sentence were shown on computer screen. Subjects were asked to rate how good the sentence describes the picture. Subjects rated also their fatigue before and after the test and answered some general questions about health, wake-up time etc.

Our results show that the effect of fatigue on the spatial perception differs according to the meaning of preposition. It was proper that tired subjects choose less acceptable ratings for prepositions "virs" (above) and "uz" (on), but for prepositions "zem" (under), "tuvu" (next to) and "pa labi" (to the right) fatigued subjects choose more acceptable ratings. Results show that fatigue no impacts on spatial language and spatial cognition. Logan and Sadler (1996) in their study elaborated spatial templates for ten English prepositions. They determined the regions corresponding to good, acceptable and bad examples of each preposition. Results in present study in Latvian support *Logan and Sadler's* findings. The only difference is in case of Latvian prepositions "virs" and "uz" having different meanings than the corresponding prepositions in English. The region of acceptability is very small in case of "uz" (on) which is different from the initial English version of the test. According to the data analysis we cannot observe any impact of the daytime (when the test is conducted) on the test results.

Acknowledgment

This study is supported by ESF No.2013/0021/1DP/1.1.1.2.0/13/APIA/VIAA/001.

Reference

Logan, G. D., Sadler, D. D., A Computational Analysis of the Apprehension of Spatial Relations, In: *Language and Space*(P.Bloom, M.A.Peterson, L.Nadel and M.Garret Eds.) MIT Press, Cambridge, p.493-529.

Speeded verification test in spatial perception under mental fatigue condition

Elina Vevere^{1*}, Jurgis Skilters², Vsevolod Liakhovetckii^{1,3}, Gunta Krumina¹

¹University of Latvia, Department of Optometry and Vision Science, Riga, Latvia

²University of Latvia, Center for the Cognitive Sciences and Semantics, Riga, Latvia

³Pavlov Institute of Physiology, Russian Academy of Sciences, St.Petersburg, Russia

*E-mail: elina-vevere@inbox.lv

Introduction

Mental fatigue occurs during monotonous work. It impairs physical performance, which may become apparent of sleepiness, lethargy, attention and concentration decline (Marcora *et al.*, 2009). Mental fatigue affects making decisions, performing tasks that require constant concentration. Our research aim is to determine how mental fatigue affects human visual spatial perception and reaction time.

Method

The research included 43 participants between the ages of 18-35 years. Participant's task was to give the shortest possible time response whether statement conform with image. The statement had two prepositions in Latvian - "virs" (above) and "zem" (below). Participants had to assess 192 steps - the statement and image. At the end they had to answer on a questionnaire about fatigue and health.

Results

The research assessed the impact of statement on human reaction time. When statement ("true") and the layout of objects are matching, participant gives faster response than if the statement is not coincide with picture. Assessing the effects of time of day, data shows longer response time at the morning and evening, and this relation is observed both at a "true" and "false" statement. The least mistakes (about 4%) of given replies, was in the morning hours. The other times of the day data did not differ statistically. If we appreciate the effects of fatigue on the reaction time and mistakes, then a strong correlation can't be observed. In preposition "below" case reaction time is longer than in the preposition "above" case, as well as mistakes have been realized in preposition "below" case.

Conclusion

Longer reaction time is in the morning, where fewer mistakes are made. During the day people faster bind together statement with image, but the mistake proportion increases. Shorter response reaction time and less mistakes are in response to the statement "above".

Latvian language prepositions have small impact on reaction time. Only still remain unexplained "above" and "below" prepositions statistically significant difference in reaction time and mistakes quantity.

Acknowledgement

This study is supported by ESF No.2013/0021/1DP/1.1.1.2.0/13/APIA/VIAA/001.

References

[1] Marcora, S.M., Staiano, W., Manning, V. Mental fatigue impairs physical performance in humans, *Journal of Applied Physiology*, 106, p.857-864 (2009).

Impact of mental fatigue on perception of biological motion

Liva Arente¹, *, Jurgis Skilters², Vsevolod Liakhovetckii^{1,3}, Gunta Krumina¹

¹*University of Latvia, Department of Optometry and Vision Science, Riga, Latvia*

²*University of Latvia, Center for the Cognitive Sciences and Semantics, Riga, Latvia*

³*Pavlov Institute of Physiology, Russian Academy of Sciences, St.Petersburg, Russia*

*E-mail: liva.arente@inbox.lv,

Introduction

The drivers at the wheel must be able to assess what is happening on the road on different weather conditions to prevent traffic accidents. Fatigue affects the driver's attention. It could be decreased and it can improve the detection of biological motion. The purpose of our research is to evaluate mental fatigue impact on ability to detect biological motion. Our tasks were: (1) to evaluate effect of different noises on detection of biological motion, (2) to evaluate the effect of day-time on test performance, (3) to estimate the threshold of noises when biological motion is detected in the condition of mental fatigue.

Method

Stimuli consisted from biological and non-biological motion in noise presented on computer screen. Non-biological motion was close to human gait and moving in same frequency. 38 subjects in age 18-55 participated in this study. Test began with noise which is represented by 2000 dots. Points decreased gradually - 100 per second. Subject task was to perceive motion and to detect what kind of motion it was (normal or scramble). Biological or non-biological motion every time was presented on different areas of screen. There were biological motion (right, left, forward) and five noises (left-right in 45 degrees, right-left in 45 degrees, top-down, random and quasi-random). To make task more difficult contrast was reduced.

Results

Biological motion perception was dependent on time of the day. The threshold of noise when was possible to detect motion in evening was 1358 dots (+/-26 dots), while in other times average threshold was 1559 dots (+/-9 dots). The threshold of biological motion perception in random and quasi-random noises were lower than in top-down, left-right and right-left in conditions. We could not find the impact of fatigue on threshold of weather simulated noises, but in case of random and quasi-random noises the tired subjects showed better results as non-tired subjects. We could not find the difference between the detection of normal biological motion and scramble motion in different conditions of noises.

Acknowledgement

This study is supported by ESF No.2013/0021/1DP/1.1.1.2.0/13/APIA/VIAA/001.

The effect of blur adaptation on blur sensitivity

Anete Pausus*, Peteris Cikmacs, Gunta Krūmina

Department of Optometry and Vision Science, University of Latvia, Kengaraga 8, Riga, Latvia, LV-1063

*E-mail: anete.pausus@lu.lv

Blur perception is an important part of visual perception and accommodation control. [1] The source blurring method [2] was used to determine various thresholds of blur perception as blur level was increased (just noticeable blur and unrecognizable optotype perception threshold) or decreased (clear image perception, optotype orientation, recognition threshold). Gaussian low-pass filter with different blurring disc diameters was used to simulate image blurring. The effect of additional adaptation to optical defocus (1,0 D simulated myopia) was evaluated.

Results showed that thresholds decreased on average by 27 - 48 % for different blur perception aspects for myopic participants after adaptation. For emmetropic participants thresholds decreased on average by 10 - 42 % after adaptation (see Fig. 21).

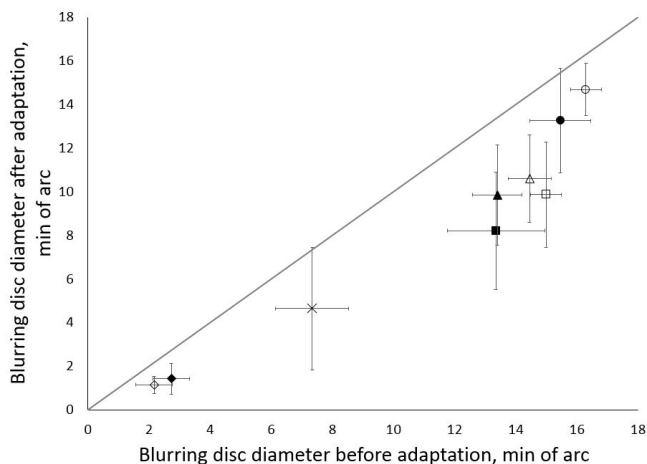


Figure 19: Blur perception thresholds for myopes (black markers) and emmetropes (white markers) before and after adaptation to 1,0 D simulated myopic optical blur. Circles - orientation, triangles - recognition threshold, squares - unrecognizable optotype, cross - clear image, diamonds - just noticeable blur threshold

References

- [1] Smith G, Jacobs RJ, Chan CDC, *Optom Vi Sci.* **66**, 430-435 (1989)
- [2] Dehnert A, Bach M, Heinrich SP, *Ophthalmic Physiol Opt.* **31**, 625-631 (2011)

Acknowledgement

This study is supported by

ESF project No.2013/0021/1DP/1.1.1.2.0/13/APIA/VIAA/001

Mental rotation test in condition of fatigue

Kristiana Ozola^{1*}, Jurgis Skilters², Vsevolod Liakhovetckii^{1,3}, Gunta Krumina¹

¹University of Latvia, Department of Optometry and Vision Science, Riga, Latvia

²University of Latvia, Center for the Cognitive Sciences and Semantics, Riga, Latvia

³Pavlov Institute of Physiology, Russian Academy of Sciences, St.Petersburg, Russia

*E-mail: ozola.kristiana@gmail.com

Introduction

Mental rotation is the ability to rotate two and three-dimensional objects in your mind. Mental rotation of three-dimensional objects have been experimentally studied since 1971 when R.Shepard and J.Metzler [1] found that if the angle of rotation increases, then the reaction time for detecting it increases as well. The aim of our study is to examine the possible impacts of fatigue on the ability of mental rotation. Our study has 2 main aims: 1) to estimate a possible correlation between the particular time of day and reaction time in mental rotation task of 2D and 3D objects; 2) to assess the possible impact of fatigue on the reaction time in mental rotation task.

Method

To evaluate reaction time for recognizing rotated objects (whether they do or do not match each other) we have constructed a special digitized test that consists of 256 object pairs (128 two- and 128 three-dimensional). When the pair of objects is shown on screen the participant has to indicate whether the object is the same (but rotated) or whether it is the mirror image of the same object.

Results

In case of 2D and 3D mental rotation reaction times are longer for mental rotation of mirrored objects. The error rate is higher in evaluating 3D objects than the 2D objects. We support Shepard and Metzler's (1971) observation that if the angle of rotation increases, the reaction time for evaluating object pairs increases as well. If the angle of rotation and the speed of detecting the rotation are compared in 2D object, reaction time for some types of figures is faster. According to our results rotation of 3D objects produces more errors if the test is conducted within the first 5 hours after waking up or since 15 hours of being awake. However, we are not able to observe any significant effects of fatigue on the mental rotation task.

Conclusion

The reaction time of 2D figures is longer in the morning, the 3D image has the longest reaction time in the morning and by night. The highest error rate occurs in the morning time (shortly after waking up). We were not observe any impact of fatigue on the mental rotation task.

Acknowledgement

The study is supported by ESF No.2013/0021/1DP/1.1.1.2.0/13/APIA/VIAA/001.

References

[1] Shepard, R., Metzler, J. Mental Rotation of Three-Dimensional, *Science*, 171(3972), p.701-703 (1971).

Experiment session duration effect on chromatic sensitivity threshold

Renars Truksa^{1,*}, Janis Dzenis¹, Gunta Krumina¹

¹ *Department of Optometry and Vision science, University of Latvia, Kengaraga 8, Riga, Latvia, LV-1063*

**E-mail: reenaars@inbox.lv,*

Colour vision research results are useful for science and as well for everyday life. Studies with patients who have altered colour vision give opportunity to find more about mechanisms which governs our colour perception. Knowledge obtained in experiments allows develop methods to determine changes in chromatic sensitivity during the time which might be useful in medicine. Aim of current research to find out whether prolonged colour vision experiment sessions have any influence on chromatic sensitivity thresholds. In order to prove or reject hypothesis we offer two types of colour vision test designs. We suggest static and dynamic colour vision tests. Static colour vision test share design features with HRR colour vision test. Test stimuli are created digitalizing HRR test plates by employing picture segmentation and edge detection algorithms. Dynamic colour vision test shares some design features with Colour and Assessment colour vision test with exception that test background is created in way which doesn't allow artefact figures. Equal luminance clusters - artefact figures may draw patient attention from main task and lower chromatic threshold therefore artefact figures are excluded from test stimuli. Before each experiment session patient chromatic sensitivity is measured in 6 chromatic directions and corresponding chromatic thresholds are obtained. Testing procedure is designed in way that excludes possibility to adapt for specific type of colour stimuli either gain skills which might improve results. After mentioned procedures colour vision testing is continued by using constant stimuli method. When fixed number of stimuli are presented series of threshold stimuli are shown. Results obtained from these experiments hopefully will clarify whether experiment session duration have any effect on person colour vision performance.

Acknowledgement:

This study is supported by ESF project No.2013/0021/1DP/1.1.1.2.0/13/APIA/VIAA/001.

The Effect of Fatigue on Eye Movements and Metaphor Comprehension in Reading

Inga Jurcinska^{1,*}, Ilze Laicane¹, Jurgis Skilters², Gunta Krumina¹

¹*Department of Optometry and Vision Science, University of Latvia, Kengaraga 8, Riga, Latvia, LV-1063*

²*Department of Communication Science/ Center for Cognitive Sciences and Semantics, University of Latvia, Lomonosova 1A, Riga, Latvia, LV-1019*

**E-mail: ingaj114@gmail.com,*

Two basic components of eye movements are the saccades and fixations. The average fixation duration in reading is 225-250 ms, whereas fixation durations can be extended between 150 ms and 500-600 ms (or even more). Skilled readers make about 10-15 percent eye movements as backward saccades, called regressions. Most regressions refer to the previous word, although when the text is exceptionally difficult, more long-range regressions can occur referring to previously read parts of the text [1]. Metaphors are different than the literal language in that they critically involve previous experience, which enables to understand the metaphorical meaning. Furthermore, metaphors help to express ideas that are difficult or impossible to express literally. Previous experiments with eye movement recordings show that more familiar metaphors are read faster than less familiar metaphors [2].

The aim of the current research is to analyze main characteristics of the eye movements (fixation duration, regressions and dispersion) and the effect of fatigue on the eye movements in reading and comprehending metaphors.

Three different texts containing simple, more complex metaphors and no metaphors were used. To analyze the comprehension and to motivate the participants, several questions about the context were asked after reading every text. Six (2 fatigued and 4 not fatigued) students participated in the experiment. All participants were native Latvian speakers with normal vision at near. Monocular eye movements were recorded with an iView HiSpeed video-based eye tracker. Data analysis was performed with BeGaze and Microsoft Excel.

The average fixation duration when reading texts without metaphors was 259ms, whereas the average fixation time when reading texts with complex and simple metaphors texts was respectively 254ms and 243ms. The results also demonstrate that fatigue had an impact on cognitive processing when reading all three texts. The comprehension was similar to both fatigued readers and participants who were not tired (83 and 77 percent of answers were correct) but the task execution time was increased in fatigued participants. Fatigued participants had almost twice as much regressions than the non-fatigued group. Most regressions were made to the previous word, although sometimes regressions were performed to the beginning of the row.

Study is supported by ESF project No.2013/0021/1DP/1.1.1.2.0/13/APIA/VIAA/001

References

- [1] Rayner, K., Eye movements and attention in reading, scene perception, and visual search. *The Quarterly Journal of Experimental Psychology*, **62(8)**, 1457-1506, (2009)
- [2] Blasko, D. G., Reading and Recall of Metaphorical Sentences: Effects of Familiarity and Context. *Metaphor and Symbol*, **2(4)**, 261-285, (1997)

Investigation of EDFA performance in 8 channel WDM transmission system.

Ingrida Lavrinovica¹, Jurgis Porins¹

¹*Institute of Telecommunications, Riga Technical University, Azenes st.16/20, Riga, Latvia, LV-1048*

**E-mail:ingrida.lavrinovica_1@rtu.lv*

Erbium Doped Fiber Amplifier (EDFA) obtained a wide range of scientific and commercial applications in optical fiber communication systems. It has been considered as an attractive solution because of several major advantages - low loss optical window of silica based fiber (1525-1565 nm), high energy efficiency (more than 50 %) and time constant enough to cover modulation noises. However, the presence of amplified spontaneous emission (ASE) limits the peak gain. EDFA gain spectrum is wavelength dependent and it applies as SNR differential between channels after passing through a cascade of EDFA [1, 2].

In this report the performance of an EDFA in a 40 Gbit/s 8 channel DWDM transmission system with NRZ-OOK modulation format and 100 GHz channel spacing was investigated. The experimental part was focused on optimization of EDFA parameters. Optimal length depends on doping level and pump power, therefore different doped fiber lengths (10m, 15m, 20m, 25m, and 30m) and excitation source power (200mW, 300 mW, 400mW, 500 mW) were used in order to reach the highest amplification value (see Fig.1). Gain was measured at each DWDM channel.

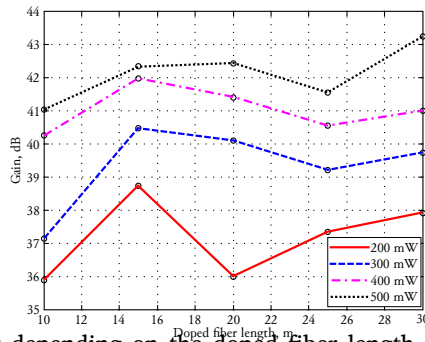


Figure 20: Gain plot depending on the doped fiber length for each pump power is displayed for the 8 channel DWDM transmission system

The obtained results have shown that at the pump power of 400 mW and 500 mW EDFA has already reached its saturation regime and gain is almost constant: 41-42 dB. The highest gain of 43 dB was got if doped fiber length is chosen to 30m. In order to reach higher gain values –longer fibers and more powerful excitation sources should be used.

References

- [1] H. K. Kim, S. Y. Park, D.H. Lee, C. S. Park, Design and control of Gain Flattened Erbium Doped Fiber Amplifier for WDM application, ETRI Journal **Vol.20**, 28-38 (1998).
- [2] Bishnu Pal (ed.), *Frontiers in Guided Wave Optics and Optoelectronics* (Intech, 2010).

Dispersion influence considerations in fiber optics transmission system

Piyush Bajpayee^{1,*}

¹Riga Technical University, Institute of Telecommunications, Azenes 16/20, Riga, Latvia, LV-1048

*E-mail: piyush.bajpayee@rtu.lv,

Next generation optical communication systems require high capacity, better spectrum efficiency and more system flexibility. To achieve this target lots of limiting factors have to be taken into account when analyzing signal transmission in optical fiber. In the linear propagation regime (optical power around 0 dBm) the main problem is dispersion. Dispersion broadens the optical pulses propagating down the fiber line. In general, the extent of pulse broadening depends on the width and the shape of initial pulses [1]. Therefore for different modulation formats and data transmission rates this influence have to be studied to choose the most desired set of measures to decrease this distortion.

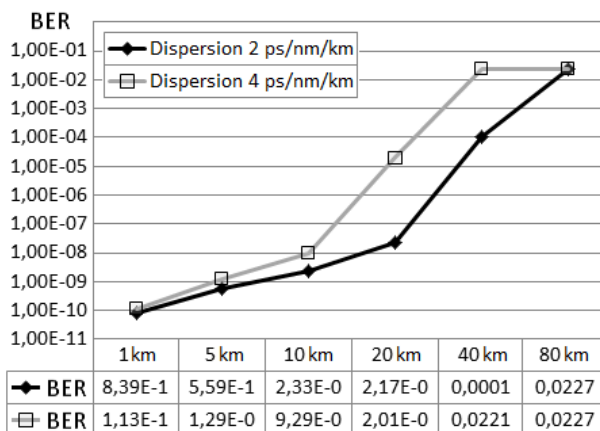


Figure 21: Changes in 10 Gbps optical signal BER depending on fiber length in kilometers for two dispersion coefficients 2 and 4 ps/nm/km.

In this research the author analyzes the influence of dispersion to 10 Gbps optical signal with return to zero and non-return to zero modulation formats. As it can be seen in Fig.21 the two different dispersion coefficients (2 and 4 ps/nm/km) have a different influence to signal bit error ratio (BER). When dispersion coefficient is higher signal BER decreases faster depending on the fiber line length, because pulse broadening is more pronounced. Dispersion compensation can be used to overcome this undesirable broadening.

References

[1] G. P. Agrawal, Fiber-Optic Communication Systems Fourth edition, John Wiley & Sons, 2010.

[illegible]

Notes – DOC 2015, Riga, April 8-10, 2015

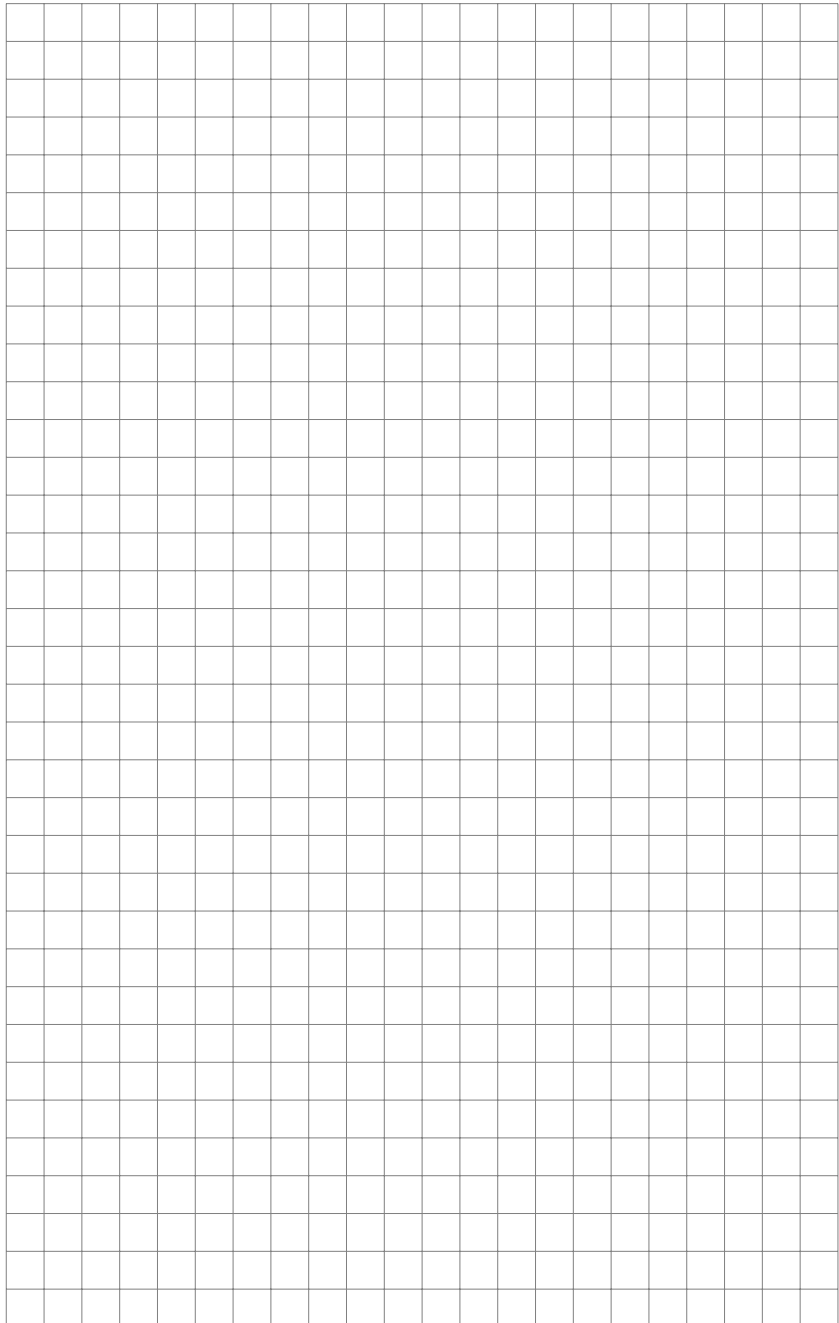
This image shows a full page of blank graph paper. The grid consists of small, uniform squares formed by thin, light gray lines. There are no margins, text, or other markings on the page.

This image shows a full page of blank graph paper. The grid consists of small, uniform squares formed by thin gray lines. There are no margins, text, or other markings on the page.

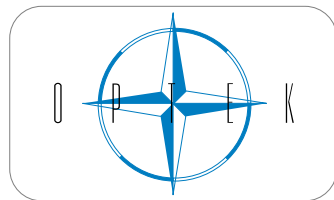
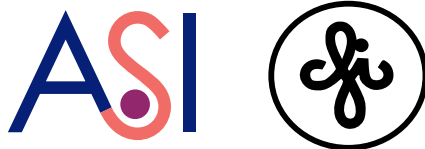
Notes – DOC 2015, Riga, April 8-10, 2015

This image shows a full page of blank graph paper. The grid consists of small, uniform squares formed by thin, light gray lines. There are no margins, text, or other markings on the page.

Notes – DOC 2015, Riga, April 8-10, 2015



DOC 2015 is Organized and Supported by:



University of Latvia



ISBN978-9934-517-80-8



9 789934 517808